Mémoire, Partim A, COLLÉGIALITÉ

Auteur : de Krahe, Jérémy
Promoteur(s) : Jérôme, Christine
Faculté : Faculté des Sciences
Diplôme : Master en sciences chimiques, à finalité approfondie
Année académique : 2024-2025
URI/URL : http://hdl.handle.net/2268.2/22656

FACULTY OF SCIENCE

Department of Chemistry

Center for Education and Research on Macromolecules (CERM)

Prof. Christine Jérôme

Development of techniques for scaffolding amorphous polyphosphoesters in nanofiber fabric

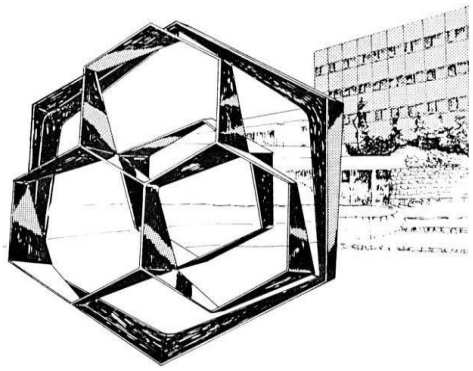

Thesis submitted by

De Krahe Jérémy

For de degree of Master of Chemical Science

Academic Year 2024-2025

ACKNOWLEDGMENTS

First of all, I would like to thank **Prof. Christine Jérôme** for allowing me to carry out my master's thesis at CERM, as well as for the corrections made to my thesis and the ideas shared for experiments to achieve my goal.

I would also like to thank all the members of my jury: **Prof. Christine Jérôme, Dr. Antoine Debuigne, Dr. Raphaël Riva, and Dr. Oscar Rabaux** for taking part in the evaluation of my work.

I would like to especially thank **Raphaël Riva** for supervising me during this thesis. You have provided invaluable help and a considerable amount of new skills and knowledge, both from a theoretical and practical point of view, as well as in terms of the transversal skills necessary for scientific research.

I would also like to particularly thank **Charlotte Dannemark**, who greatly contributed to my practical training, whether it was for synthesis or electrospinning, and who, on numerous occasions, always took the time to help me, whether for practical issues, to find a product, or for electron microscopy. Thank you also for the always interesting discussions, the good mood, and the relaxing atmosphere in the laboratory (referring to the music).

I thank **all the members of CERM**. I greatly appreciated the spirit of mutual help and the great atmosphere that prevails at CERM. Whenever I had a question or needed assistance, whether it was for rheometer measurements, performing an NMR outside the scheduled slots, getting information for the SEM, and many other things, I was always helped. I will never thank enough for the help provided to me throughout the year. CERM gave me a fantastic first experience of working in a research laboratory.

Ce mémoire marque la fin d'un long parcours étudiant. Je tiens donc également à remercier tous ceux qui m'ont suivi de près, soutenu et aidé tout au long de ce parcours, et qui m'ont guidé dans la bonne direction pour atteindre cet objectif de réaliser un Master en sciences chimiques. Je tiens à remercier tout particulièrement l'Institut Sainte-Claire de Verviers, les éducateurs, les enseignants et les aides externes de l'école qui m'ont donné l’opportunité de suivre cette voie.

TABLE OF CONTENTS

RESUME

Dans de nombreuses applications biomédicales telles que l'administration de médicaments et l'ingénierie tissulaire, il est nécessaire d'utiliser des polymères répondant à certaines exigences telles que la biocompatibilité avec le corps humain et la biodégradabilité. Autrement dit, le polymère utilisé ne doit pas être reconnu comme corps étranger par le corps humain et ne doit pas avoir de toxicité potentielle.De plus, dans le cadre de l'ingénierie tissulaire, le matériau polymère utilisé doit pouvoir adhérer et répondre de manière optimale à son application et donc posséder une structure et des propriétés mécaniques adéquates. Dans le cadre de cette thèse, les polyphosphoesters (PPEs), qui sont une classe de polymères répondant parfaitement à des propriétés de biocompatibilité et de biodégradabilité, sont étudiés. Les PPEs ont effectivement une structure très similaire à celle des brins d'ADN, ce qui les rend biocompatibles, et les liaisons ester sont facilement hydrolysées, ce qui les rend facilement dégradables. Cependant, dans le cadre de l'ingénierie tissulaire, il faut pouvoir mettre en œuvre les PPEs avec une structure adéquate à l'objectif visée. Dans le cadre de cette thèse, l'objectif est de pouvoir créer un tapis de nanofibres de PPEs. Le fait qu'il s'agisse de structures nanofibre augmente l'adhésion et la surface de contact avec le tissu biologique. Pour créer cette structure, il est nécessaire d'utiliser des techniques de mise en œuvre de structures polymères telles que l'électrofilage qui est la technique utilisée dans cette thèse dans l'objectif de créer des structures nanofibres.

Deux projets de recherche expérimentale ont été menée dans le cadre de cette thèse. La première recherche vise à créer un fil polymère par électrofilage. Pour ce faire, il est indispensable de contrôler la viscosité des solutions de polymères. La viscosité influence directement la formation des nanofibres et la qualité du tissu final. Ainsi, des expériences sont réalisées pour ajuster la viscosité des solutions de polymères, en faisant varier différents paramètres tels que la nature des polymers et la masse molaire.

La deuxième recherche porte sur la fixation du tissu de nanofibres au collecteur. Cette étape est importante pour garantir la solidité et la structure du tissu final. Pour ce faire, la technique étudiée est une fixation par photoréticulation du polymère. Il faut dans un premier temps s'assurer que la réaction de photoréticulation est bien réalisée et dans un deuxième temps améliorer la vitesse de fixation pour que le polymère soit fixé directement après son dépôt sur le collecteur et ainsi pouvoir former une structure de nanofibres.

En combinant ces deux investigations expérimentales, la thèse vise à optimiser le procédé d'électrofilage pour la fabrication de tissus en structure fibreuse à base de polyphosphoesters. Les résultats de ces expériences fourniront des informations précieuses pour la conception et la production de matériaux biomédicaux, avec des applications potentielles en médecine régénérative, dans les implants et les dispositifs médicaux.

ABSTRACT

In the context of numerous biomedical applications such as drug delivery and tissue engineering, it is necessary to use polymers that meet certain requirements such as biocompatibility with the human body and biodegradability. This means that the polymer used must not be recognized as a foreign body by the human body and must not pose potential toxicity. Additionally, in the context of tissue engineering, the polymer material used must be able to adhere and meet the requirements of its application, thus requiring adequate structure and mechanical properties. In this thesis, polyphosphoesters, a class of polymer that perfectly meets the properties of biocompatibility and biodegradability, are studied. Polyphosphoesters indeed have a structure similar to DNA strands, making them biocompatible, and ester bonds are easily hydrolyzable, making them easily degradable. However, in the context of tissue engineering, it is still necessary to be able to implement PPEs. The objective of this thesis is therefore to create a nanofiber mat of PPEs. The nanofiber structure increases adhesion and the contact surface with biological tissue. To create this structure, it is necessary to use polymer processing techniques such as electrospinning, which is the technique used in this thesis to create nanofiber structures.

Two experimental studies are undertaken to achieve this objective. The first research aims to create a polymer filament using electrospinning. To do this, it is essential to control the viscosity of the polymer solutions. Viscosity directly influences the formation of nanofibers and the quality of the final tissue. Thus, experiments are conducted to adjust the viscosity of the polymer solutions by varying parameters such as the nature of polymers and molar mass.

The second research focuses on attaching the nanofiber tissue to the collector. This step is important to ensure the strength and structure of the final tissue. For this, The technique studied is polymer photo-crosslinking. It is therefore necessary, first, to ensure that the photo-crosslinking reaction occurs, and secondly, to improve the fixing speed so that the polymer is fixed directly after deposition on the collector, thus creating a nanofiber structure.

By combining these two experimental studies, the thesis aims to optimize the electrospinning process and for the manufacture of tissue from polyphosphoesters with a fibrous structure. The results of these experiments will provide valuable information for the design and production of advanced biomedical materials, with potential applications in the field of regenerative medicine, implants, and medical devices.

LISTE OF ABBREVIATIONS

PPEs: Poly**P**hospho**E**ster**s**

DSC: Differential **S**canning **C**alorimetry

NMR: Nuclear **M**agnetic **R**esonance spectroscopy

SEC: Size **E**xclusion **C**hromatography

GPC: Gel **P**ermeation **C**hromatography

DBU: 1,8-**D**iaza**B**icyclo**[**5.4.0]**U**ndec-7-ene

TU: [Cyclohexyl-3,5-bis(trifluoromethyl)phenyl]**T**hio**U**rea

THF: Tetra**H**ydro**F**uran

BenHP: Poly(**Ben**EP-stat-**H**E**P**)

BenBP: Poly(**Ben**EP-stat-**B**E**P**)

BEP: Butyl **E**thyl **P**hosphate

BenEP: But**en**yl **E**thyl **P**hosphate

HEP: Heptyl **E**thyl **P**hosphate

BenP: But**en**yl cyclic **P**hosphate monomer

BP: Butyl cyclic **P**hosphate monomer

HP: Heptyl cyclic **P**hosphate monomer

LISTE OF FIGURES

1. Introduction

1.1 Tissue engineering

In the late 1980s, the concept of "tissue engineering" was defined to gather under an unique denomination the researches aiming to create artificial tissues or restoring, maintaining and improving existing tissues or organs [1-5]. Tissue engineering encompasses three main approaches: the implantation of isolated cells or cell surrogates in the body, delivery of tissue-inducing substances, and placing cells in an appropriated scaffold, which is the most common approach scaffolding being a reliable method to mimic the physiological environment [6].

Biomaterials can be grouped into several categories according to their structural, chemical and biological properties, such as ceramics, glasses or polymers. Among them, polymers are ideal candidates for the design of scaffolds due to the ability to finely control structural, mechanical, and chemical characteristics reproducibly[7]. The design and fabrication of polymer-based scaffolds are innovative areas of biomaterial researches in tissue engineering and regenerative medicine[8]. To be considered as matrices, selected biocompatible polymers must have a specific structure that promote cell-biomaterial interactions and cell adhesion, allow for sufficient transport of gases, nutrients, and regulators, and have a degradation rate similar to the rate of tissue regeneration[6-11].

The design of the polymer scaffolds is therefore a key aspect of tissue engineering. Among the various polymer structures explored, polymer hydrogels and fibrous materials stand out as particularly promising. Indeed, hydrogels are three-dimensional networks of hydrophilic polymers that are able to absorb large amounts of water while maintaining their structure. Hydrogels can be made from synthetic or natural polymers, crosslinked by covalent or non-covalent bonds[11,12]. The water-absorbing ability confers to hydrogels a high porosity and optimal permeability, which are crucial parameters for nutrient diffusion and the removal of metabolic waste. Additionally, their flexibility and similarity to the natural extracellular matrix create a favorable environment conducive to cell proliferation and differentiation[12].

Although hydrogels are often applied in tissue engineering[13-15], they often lack the fibrillar structure necessary for the extracellular matrix of the tissue for which the biomaterial is designed[16]. It is therefore necessary to develop 3D scaffolding techniques in order to obtain a suitable architecture for the biological tissue.

For fibrous materials, Smith, I. O., et al.[6] showed that nanofiber structures increase cell proliferation, differentiation, and adhesion to cellular tissues, mainly due to their high surface-to-volume ratio. Polymer nanofibers have thus attracted increasing interest over the past decade. In the context of nanostructured materials, a nanofiber is generally defined as a fiber with a diameter of less than 100 nanometers. However, the term "nanofibers" is also used to refer to fibers with a diameter of less than 1000 nanometers (or submicrometers) when produced via ultrafine fiber fabrication techniques[17].

Researches on fabrication methods is an important area of study for polymer nanofibers and has attracted considerable interest in both academia and industry. Various processes, such as electrospinning, melt blowing, phase separation, self-assembly, and template synthesis, have been employed to produce polymer nanofiber mats suitable for different applications[17]. Among these techniques, electrospinning stands out as the most widespread and preferred, as it is both simple, economical and capable of generating continuous nanofibers from various materials, ranging from polymers to ceramics. Moreover, electrospinning appears to be the only process with development potential for large-scale production of continuous nanofibers for industrial applications.

1.2 Soft tissue engineering scaffolding technique: Electrospinning

1.2.1 Principle of electrospinning

For many years, electrospinning technique is a relevant method for the manufacturing of polymer scaffolds in tissue engineering characterized by the implementation of a polymer as a nanofiber mat. Specifically, a voltage is applied between the metallic needle of a syringe containing a polymer solution and a conductive collector (Fig.1).

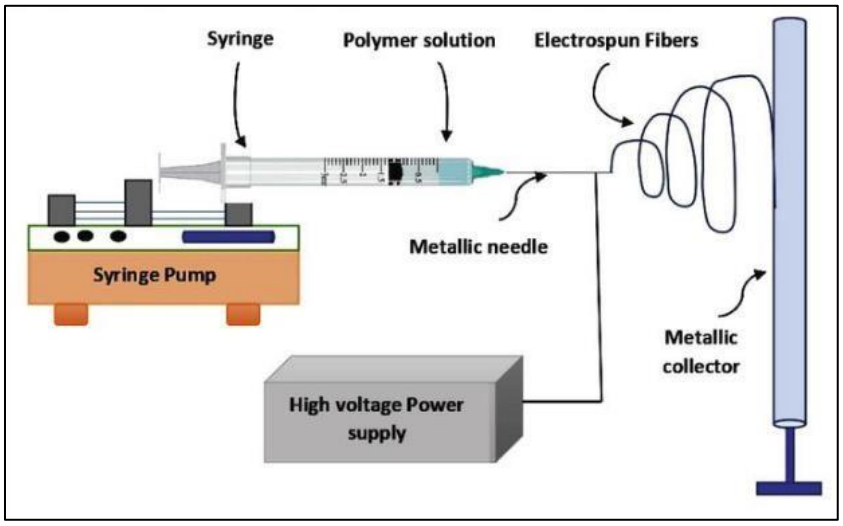

Figure 1: The technique of electrospinning[18].

Physically, when the polymer solution comes out of the needle, the surface tension force is largely counterbalanced by an electrostatic repulsion phenomenon, so the teardrop shape no longer minimizes the surface energy, and a polymer thread is formed from the needle to the collector[18,19].

The parameters that determine the function and final architecture of the nanofibers can be divided into three categories[19]:

Parameter of electrospinning:

- **The voltage between the metal needle and the collector:** The higher the voltage, the greater the flow rate of the electrospun jet. A high voltage will also tend to lengthen the fiber and therefore reduce its diameter.

- **The needle-to-collector distance:** The distance between the needle and the collector influences the electric field and the diameter of the fiber. A distance of 10 to 15 cm is common in the laboratory, allowing the solvent to evaporate. Increasing the distance reduces the diameter of the fiber until a certain threshold is reached, at which point the diameter increases again. There is therefore an optimum distance where the diameter of the fiber is minimal.

- **Solution flow rate in the needle:** The flow rate of polymer into the needle should match the amount of solution leaving to minimize variation in fiber diameters. A too high flow rate will increase fiber diameter and may create droplets or ribbons, although beads may be advantageous for some applications. A too low flow rate can interrupt spinning or cause a wide variation in fiber diameters.

- **Collector shape:** The shape of the collector influences the local nanofibers density and thus mechanical properties of the final mat.

Solution Parameters:

- **Electrical conductivity:** Increasing the solution's conductivity, for example by adding ions through salts, accelerates the jet at the needle outlet and increases jetinstability. This improves the quality of the fibers and allows them to be drawn out further, producing finer fibers.

- **Viscosity:** Viscosity is the key parameter to allow an efficient electrospinning of a polymer dissolved in an organic solvent, particularly via its concentration in the solution. Viscosity influences fiber diameter, with high viscosity increasing fiber diameter. As will be discussed in more details in the next section, a too low or too high viscosity will respectively determine whether the solution emerges as a drop or not at all.

- **Polymer concentration:** The concentration of the solution will directly dictate the viscosity and volatility of the solvent.

- **Polymer molar mass and macromolecular architecture:** The molar mass and architecture of the polymer have a direct influence on viscosity and fiber formation during electrospinning. Regarding the structure, a high degree of chain entanglement is necessary to promote fiber formation, since long polymer chains allow for better cohesion during the electrospinning process. Therefore, long-chain polymers, which have more pronounced entanglement, promote better fiber formation. Concerning the

molar mass, The higher the molar mass, the higher the viscosity.

- **Solvent volatility:** The volatility of the solvent influences the fiber formation: rapid evaporation leads to thinner fibers and can form pores, but if it is excessive it can cause interruptions by solidifying the polymer near the needle. Evaporation that is too slow can leave fibers wet, causing them to melt on the collector and form unwanted bonds.

Ambient parameter :

- **Room temperature:** Higher temperatures reduce fiber diameter by reducing viscosity and evaporating the solvent more quickly.
- **Humidity**: The influence of humidity on electrospinning depends on whether the polymer is hydrophilic or hydrophobic when water vapor condenses. For hydrophilic polymers, this condensation slows down the formation of fibers and increases their diameter. In contrast, for hydrophobic polymers, water might create pores in the fibers through phase separation.

The electrospinning technique can offer a wide range of structures that closely mimic the natural extracellular matrix by producing scaffolds of 3 different types[16] (Fig.2):

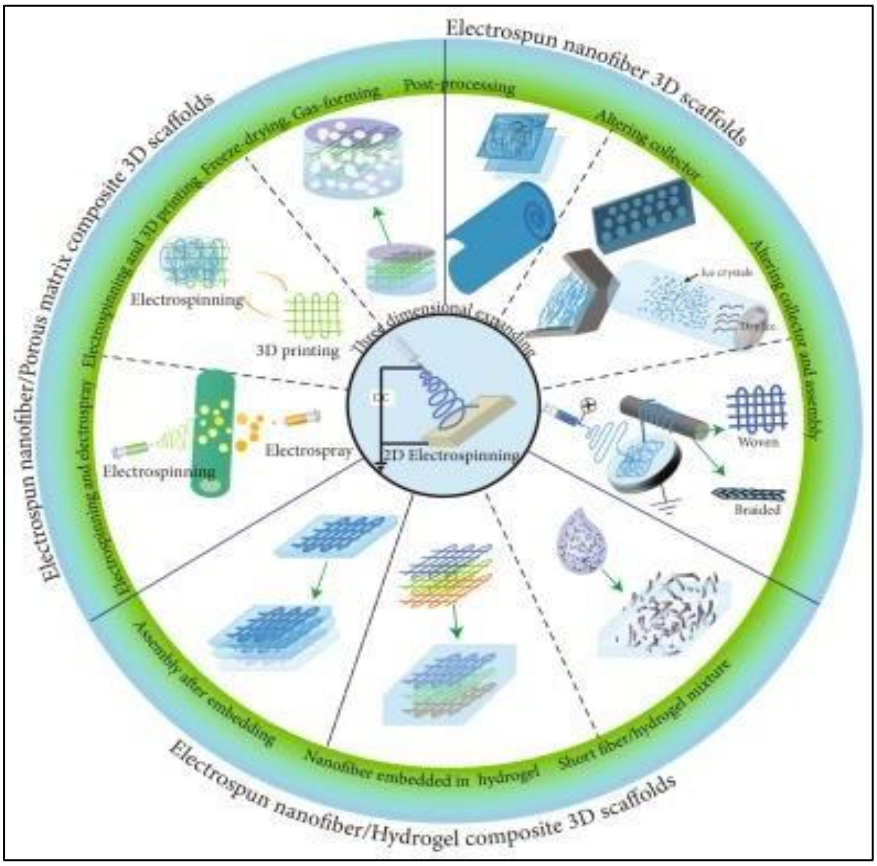

Figure 2: The summary of representative design approaches of 3D ENF-S[16].

3D electrospun nanofiber scaffolds (3D ENF-S), 3D ENF-S nanofiber/hydrogel composite scaffolds and 3D ENF-S nanofiber/porous matrix composite scaffolds offer improved characteristics such as facilitated cell infiltration, biomimetic three-dimensional fiber architecture, enhanced mechanical properties and scalable degradability. They have promising applications in the regeneration of different types of tissue, such as cartilage, bone, tendons, ligaments, skeletal muscle, nerves and cardiac tissue. These scaffolds can be adjusted to have specific mechanical properties, tailored to the needs of different tissues such as bone or cartilage. In addition, the surfaces can be functionalised to improve cell adhesion and differentiation. Advanced electrospinning techniques can create structures with aligned or oriented fibers, optimizing tissue regeneration.

1.2.2 Crucial influence of viscosity in the electrospinning process

The viscosity of a polymer solution is a key parameter for the electrospinning method that will determine more specifically the ability to form a thread.

Indeed, there are precise viscosity conditions required for a solution to be electrospun. A solution that is not viscous enough will form droplets and no thread at the end of the needle, while a solution that is too viscous will not come out of the needle, or will come out with great difficulty, leading to rapid precipitation at the end of the needle by evaporation of the solvent. It is therefore necessary to take into account each of the factors influencing the viscosity of a polymer solution. These factors are temperature, the polymer structure, the molar mass and the polymer concentration. An increase in temperature has the effect of decreasing the viscosity and vice-versa.

Concerning the molar mass, the famous Mark-Houwink relation (Eq. 1) illustrates well the fact that a higher molar mass will tend to increase the viscosity:

$$\eta = K M^{\alpha} \qquad (1)$$

With the coefficient K and α which depends on the couple (polymer/solvent) and the temperature. These parameters can be determined experimentally by expressing the Mark-Houwink equation in logarithmic form.

Finally, the polymer concentration is the most important parameter to play on the value of the viscosity given its important influence on the viscosity, the speed and the ease of preparing solutions. This parameter is discussed in detail in the following.

In several studies[20-23], authors assumed that over a range of polymer weight concentration that goes from 0% to 100% polymer, we distinguish 4 types of solution (Fig.3):

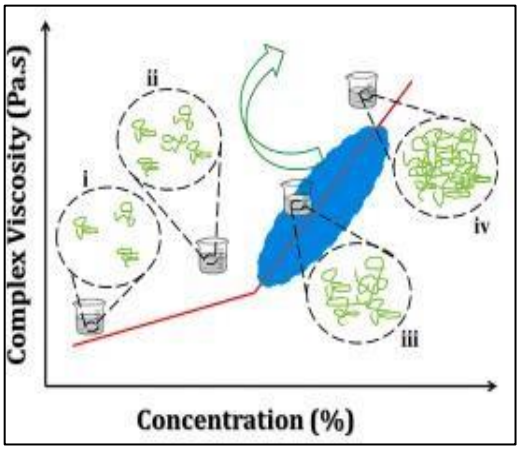

Figure 3: Schematic representation of four regimes suggested for polymer solutions: i) dilute; ii) semi-dilute I ; iii) semi-dilute II ; and iv) concentrated solution[24].

- Dilute solution: The polymer chains are largely separated by solvent molecules.The solution is characterized by a low viscosity.
- Semi-dilute non-entangled solution: The polymer chains begin to entangle, but the unentangled chain fraction is still much greater than the entangled chain fraction.
- Entangled semi-dilute solution: the non-entangled chain fraction is much less than the entangled chain fraction.
- Concentrated solution: Solution with a total entanglement of the chains. The solution is characterized by a high viscosity that tends towards the solid state.

The transition concentration of the dilute solution to the unentangled semi-dilute solution is denoted C* and is called the intrication concentration and the transition concentration of the unentangled semi-dilute solution to the entangled semi-dilute solution is denoted Ce and is called the entanglement concentration.

A polymer solution is electrospinnable at a concentration greater than or equal to Ce, with an upper concentration limit not theoretically defined beyond which the solution is too viscous. This embedding concentration can be determined by plotting the specific viscosity or complex viscosity as a function of the concentration of the polymer solution. For example, in Figure 4 taken from a study by Sandeep Kumar Tiwari et al.[21], we observe a sudden change from the slope to the entanglement concentration Ce, the intrication concentration being at a ratio C/C*=1.

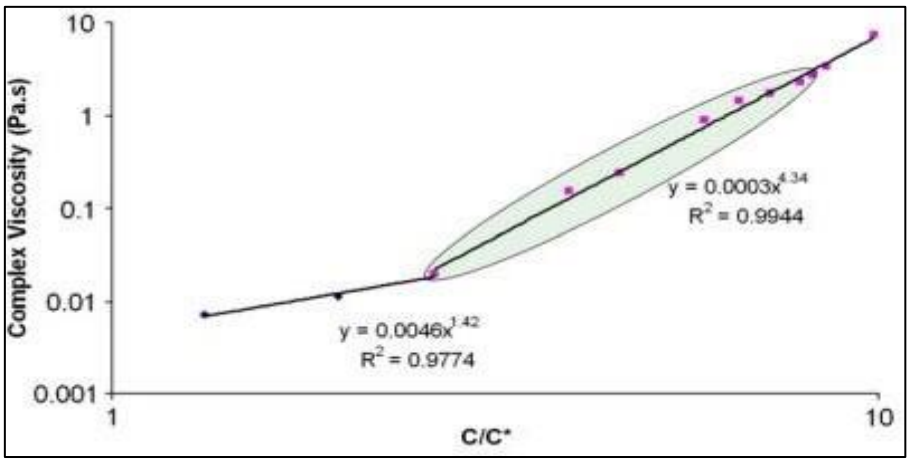

Figure 4: Dependence of PLGA solution viscosity on concentration.The oval area indicates the concentration/viscosity regime in which stable electrospinning with beadles fibers was observed [21].

In the literature, we find that the viscosity ranges of electrospinnable solutions are mainly located in an interval between 0.01 Pa.s and 100 Pa.s. Figure 5 takes the example of 4 polymers taken from the literature.

	Concentration range (% by mass)	Viscosity range (Pa.s)
PLGA[21] (Mw=152,000g/mol)	[4-12] %	[0,01-2,7]
PET-*co*-PEIBranched[22] (Mw=46,000g/mol)	[6-12] %	[10-100]
PET-*co*-PEI[22]linear (Mw= 11,700 g/mol)	>18 %	[40 - 100]
PMMA (Mw=12,470-365,700 g/mol)[25]	[5-12] %	[0,01-10]

Figure 5: Viscosity and concentration range of some electrospun polymers.

1.2.3 Parameters for forming the polymer mat to the collector

The deposition of a polymer nanofiber mat onto a collector depends on both intrinsic electrospinning parameters and the type of polymer used. Regarding parameters specifically linked to electrospinning, firstly it is crucial to maintain an adequate distance between the needle and the collector. This ensures good fiber dispersion and allows sufficient time for solvent evaporation when using polymers in solution; otherwise, fiber stability may not be ensured. Secondly, the applied voltage must be high enough to attract the fibers to the collector but not so high that it causes jet instability and poor fiber formation[26,27]. Lastly, the type of collector used is crucial; it must conduct electricity. There are collectors that are not fixed and can be rotated to induce fiber orientation during deposition [28,29].

Regarding the influence of parameters related to the polymer, it is primarily the mechanical properties that dictate how to fix the polymer in the desired structure. Indeed, whether we use a semi-crystalline polymer solubilized in a solvent or an elastomer with a T_g lower than room temperature, the techniques and means used for electrospinning are not the same. These cases are studied in the following section.

1.2.4 Study of electrospun polymers for scaffolds

A variety of synthetic and natural biomaterials, including poly(lactic-co-glycolic acid) (PLGA), poly(l-lactic acid) (PLLA), poly(caprolactone) (PCL),poly(ethylene oxide) (PEO), poly(vinyl alcohol) (PVA), gelatin, collagen, silk protein and fibrinogen have been used to form nanofibrous scaffolds for tissue engineering[11-16,18-19,30-33]. Electrospinning conditions and mat properties largely depends on the thermal characteristics of the considered polymer, as follows.

a) Electrospinning thermoplastic polymers (T_g > room temperature)

Electrospinning of amorphous or semi-crystalline thermoplastic polymers, such as poly(L-lactide-co-glycolide) (PLGA), is gaining increasing interest for biomedical applications, particularly in tissue engineering[33-35]. This polymer dissolves in organic solvents, allowing its implementation as nanofiber mat with a crystalline or glassy

structure that gives the formed fibers both stiffness and mechanical strength. The success of electrospinning of soluble thermoplastic polymers depends largely on the choice of solvents, which influence the viscosity and stability of the polymer jet. PLGA, can be dissolved in hexafluoroisopropanol (HFIP), which facilitates the formation of smooth and beadless fibers. The study of Bini et al.[36] demonstrates that a Poly(L-lactide-co-glycolide)(PLGA10:90) solution with a molecular weight of 100,000 g/mol with 7% HFIP allows the production of continuous and beadless nanofibers, thus optimizing fiber structures suitable for applications such as nerve repair. Process parameters, including polymer concentration, flow rate, applied voltage, and needle-collector distance, are essential to control fiber morphology and size. For PLGA, a concentration of 7% and an applied voltage of 12 kV produces uniform and stable nanofibers, ideal for forming tubular structures in nerve regeneration applications[36].

b) Electrospinning of semi-crystalline thermoplastic polymers (T_g < and T_m > room temperature)

PCL is a type of semi-crystalline thermoplastic polymer with low Tg (-60C°) that has also been used for tissue engineering applications in the form of nanofibers[11-16,18-19,30-33]. PCL can be dissolved in a mixture of a good solvent, such as dichloromethane, and a weaker solvent, such as dimethylformamide, creating a solution with a specific viscosity that favors the formation of smooth and continuous fibers[37]. For PCL 80,000 g/mol, a concentration of 17 wt%, with an applied voltage of about 9 kV and a flow rate of 1 ml/h, favors the production of uniform fibers exhibiting high flexibility and with diameters ranging from 0.4 to 1.4 µm[37].

A particularly promising class of polymers in the context of tissue engineering and which also meets all the criteria of degradability and biocompatibility are the polyphosphoesters (PPEs)[38-40]. They are ubiquitous in nature, found in nucleic acids (DNA and RNA) and in the form of pyrophosphates, they store chemical energy in organisms. It would therefore be obvious that these PPEs constitute an important class of materials for many applications in the biomedical sector[40]. PPEs were first electrospun in a study carried out at the Johannes Gutenberg University by Hisaschi tee[40] as part of his doctoral thesis on degradable alternatives to PEG and polyolefin. More precisely, they are semi-crystalline thermoplastic PPEs with hydrophobic characteristics consisting of long carbon chains in the main chain, Tg is -20C° and the Tm is 50C° for the PPEs illustrated in the

figure 6, with a crystallinity rate of approximately 17%.

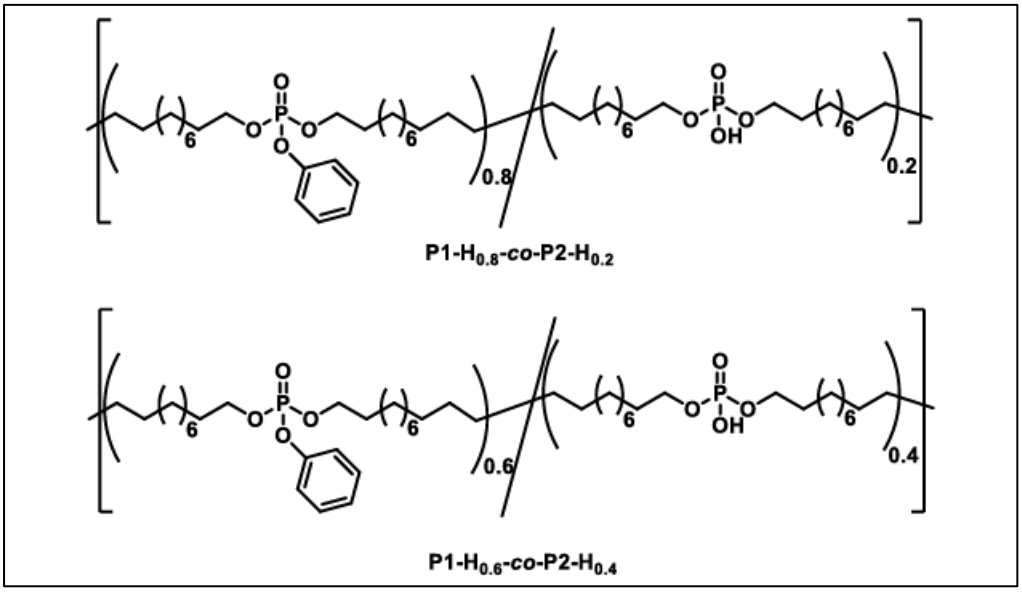

Figure 6: Structure of electrospun semicrystalline polyphosphoesters as described in the study by Hisaschi Tee[40].

The study reports that these PPEs either yielded stable fiber mats due to their good mechanical properties or a capsule-like morphology. PPEs with a molecular mass of 6000 g/mol with concentrations ranging from 2 to 10 wt% in tetrahydrofuran (THF) solutions yielded particles. To obtain fiber-like structures, a polymer concentration of at least 30 wt% is required, and concentrations of 35 wt% yield uniform fibers.

Phosphorus diester can form strong bonds with amines or salts and allows for a lower polymer concentration, due to the increased viscosity due to H-bonding. Thus, an alternative method to improve molecular cohesion was to add 1,3-diaminopropane, which allows the formation of uniform fibers at a polymer concentration of 30 wt% instead of 35 wt%. Increasing the molecular weight of PPEs to M_n 8000 g/mol allowed the production of uniform fibers in a 28 wt% polymer solution in THF, probably due to a higher degree of polymer chain entanglement. Using PPEs with a higher number of hydrogen bonding groups, a homogeneous THF solution can be obtained up to a concentration of 20 wt%, resulting in a mixture of fibers and particles. At even higher polymer concentrations, the solution transforms into an organogel. The general parameters used for electrospinning of the thermoplastic semicrystalline PPEs investigated in this study are a voltage of 10 kV, a tip distance of 8 cm, a tip inner diameter = 0.4 mm, and an ejection volume of 0.5 mL/h.

c) Electrospinning of amorphous polymers (T_g < room temperature)

Electrospinning of low-T_g amorphous polymers presents significant challenges, due to their lower viscosity and tendency to deform under stress, which complicates the stabilization of nanofibers. Various techniques have been developed to overcome these limitations, such as photopolymerization during electrospinning[41], the use of semi-crystalline and amorphous polymer blends combined with photocrosslinking[42], and the salt effect for electrospinning of amorphous polymers[43]. Shanmuganathan et al. (2014)[41] explored a method based on *in situ* photopolymerization during electrospinning of a mixture of two monomers: a tetrafunctional thiol, pentaerythritol tetrakis (PETT), and tris(4-(vinyloxy)butyl) trimellitate (TVE) to generate elastic nanofibers. The use of a mixture of trivinyl ether (PETT) monomer with a UV-active tetrafunctional thiol allowed rapid photopolymerization, generating thermoset fibers, which improves the elasticity and stability of the fibers at room temperature. Thanks to the photo-induced crosslinking, the fiber structure is strengthened before they reach the collector, thus avoiding the common deformations of amorphous polymers under low Tg. In this study, the viscosity of the initial PETT/TVE mixture was determined with a low-amplitude oscillatory shear experiment using a rheometer. A viscosity of 0.33 pa.s was determined, which is too low to perform electrospinning. Therefore, the authors added 0.6 wt% PMMA to the electrospinning solution to increase the viscosity. To this mixture, 6 wt% Igracure 2100 was added as a photoinitiator. The prepared solution was loaded into a syringe masked with black tape to block exposure to light during spinning. The flow rate of the solution was set at 1 mL/h. A potential of 20 kV was applied once the solution was visible at the tip of the needle, creating a fluid jet. At this point, the light source was turned on to harden the monomer fluid jet. The light was positioned approximately 10 cm from the fiber and directed toward the collector. The light intensity at this distance was measured to be approximately 200 mW/cm^2.

Another approach involving the blending of amorphous polymers with semi-crystalline polymers was reported by Liu et al. (2009)[42]. They combined amorphous unsaturated polyester (UPM) with poly(3-hydroxybutyrate-co-3-hydroxyvalerate) (PHBV), a semi-crystalline polymer, to form porous fibers via selective extraction. After electrospinning, the fibers were exposed to UV irradiation to induce photocrosslinking of UPM. By subsequently removing PHBV using solvents, a porous fiber structure was obtained, showing that UPM can be stabilized and structured despite its low T_g. The

electrospinning solution was carried out to have a weight percentage of UPM/PHBV of 2.5 wt% to 25 wt%, respectively, and BPO was added as an initiator. The initiator was not more than 1% based on the weight of UPM. The electrospinning process was performed at a positive voltage of 14 kV, a working distance of 14 cm and a mass flow rate of 0.8 mL/h. This method allowed to circumvent the limitations of amorphous UPM by using a semi-crystalline carrier polymer and ensuring rapid photocrosslinking thanks to the nanofiber structure of PHBV carried out before the photocrosslinking of the UPM.

A study carried out by O. Rabaux[44] showed that nanofibers diffuse UV rays in all directions, which is why photocrosslinking is significantly accelerated. The diffusion is related to the fact that the nanofibers have a size of the order of the wavelength of light. In this same study by O. Rabaux, it is interesting to note that this discovery of an increase in the kinetics of photocrosslinking thanks to the presence of nanofibers was made by photocrosslinking an amorphous PPE cast on a PCl nanofiber mat. An interesting parallel can be made here between the study by Liu et al. with the amorphous UPM mixture and semi-crystalline PHBV and the study by O. Rabaux with the amorphous PPE mixture and semi-crystalline PCl. Except that in this last situation, the amorphous polymer mixture and the semi-crystalline polymer was not electrospun.

In a study by F. Cengiz et al.[43], a polyurethane with an amorphous character was mixed in the polymer solution with a low concentration of salt, tetraethylammonium bromide (TEAB). The results of the study showed that the presence of this salt improved the conductivity of the solution, positively influencing the formation of nanofibers by improving the charge density on the polymer jet. No fibers were observed for a mass percentage of TEAB in the electrospinning solution of 0% and 0.1%, and fibers were observed for a higher mass percentage of 0.3%, 0.87% and 1.82%.

1.3 PPEs: Structure, properties and synthesis

1.3.1 Structure, biodegradability and biocompatibility.

In the context of biomedical applications such as tissue bioengineering, it is essential to have as a priority material with no toxicity for the human body, i.e. biocompatible. It is also important to consider how the compound degrades and the non-toxicity of the degradation products. These two aspects: biocompatibility and (bio)degradability, are two properties that a temporary material must combine in the context of biomedical application. Several polymers are suitable to be applied as biomaterials. Natural polymers, such ascollagen, chitosan, alginate and albulmine, are degradable materials are largely described in the literature for the manufacturing of scaffolds for tissue engineering[6,45].

Synthetic polymers are extremely valuable in the biomedical field because their physico-chemical properties can be advantageously adjusted for specific applications. These polymers are often cheaper than natural polymer-based scaffolds and can be produced in larger quantities in a uniform manner[10]. In general, they offer predictable and reproducible mechanical and physical properties, such as tensile strength, elastic modulus, and degradation rate[46]. As far as biodegradability is concerned, since 70% of the human body is made up of water, the most interesting polymers from this point of view are aliphatic polyesters, since they degrade in the presence of water, but it is necessary for them to break down into non-toxic products. Poly(lactic acid) (PLA), poly(glycolic acid) (PGA), poly(lactic-*co*-glycolic acid) (PLGA), poly(ε- caprolactone) (PCL) and poly(propylene fumarate) (PPF) are among the most commonly used synthetic polymers in tissue engineering[10,45,18]. It is important to note that finding polymers that are biodegradable, biocompatible and have adequate mechanical properties with the desired extracellular matrix is a real challenge. It is often necessary to make copolymers in order to combine many criteria as possible for tissue engineering.

A second condition is to be able to obtain a fibrillary solid support with mechanical properties that are suitable for the targeted tissue. In the case of engineering implants in harder tissues such as bone, the scaffold must present stronger mechanical properties and semi-crystalline polymers are often considered for this application [47-48]. Scaffolds based on semi-crystalline polymers are therefore no longer appropriate[49] for soft tissue

engineering implantation, as the scaffold must be elastic and flexible and it is therefore necessary to use elastic soft materials.

One last condition is to be able to create porous nanofiber structure from the selected material, especially by electrospinning[6], this technique emerging by the good control of the nanofiber structure of small diameter, high specific surface area, high porosity and a high adsorption capacity[19].

One class of polymers that is particularly promising in the context of tissue engineering and which, among other things, meets all the criteria of degradability and biocompatibility are polyphosphoesters (PPEs)[38,39].

Furthermore, their degradation can be carried out by hydrolysis with or without specialized enzymes such as alkaline phosphatase under physiological conditions[50]. The overriding advantage of PPEs over other polymers is that phosphorus is pentavalent and therefore the mechanical and chemical properties of these materials can be easily modified, ranging from amorphous, water-soluble materials to stiff, crystalline plastics, through adjustments to the backbone or side-chains. However, if these modifications lead to semi-crystalline PPEs, for example by significantly extending the carbon chain between each phosphoester unit[51], they will no longer be suitable for soft tissue engineering. Firstly, because the mechanical properties of the PPE will no longer match the mechanical properties of soft tissues, and secondly, due to the longer carbon chains, the degradation products will pose a problem of toxicity and elimination by the human body. As a result of the mechanical properties of soft tissues, it is necessary to maintain the amorphous character of PPEs.

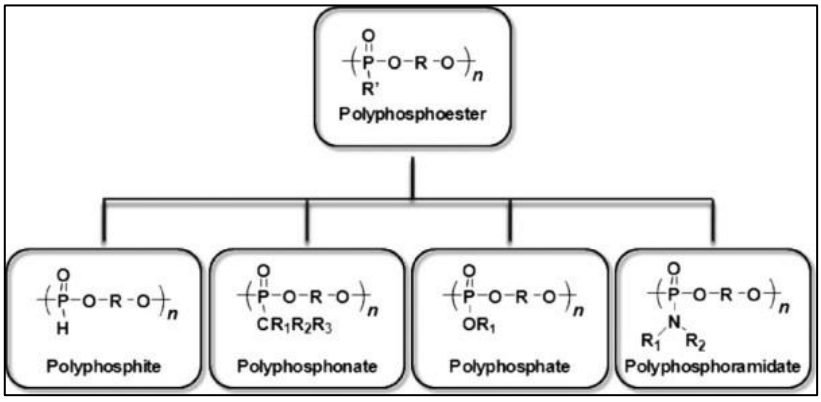

Figure 7: Overview of the subclasses of PPEs reported to date[12].

One problem with amorphous PPEs is that they have a transition temperature below room temperature (~-80C°) which, as explained in the previous sections, will pose a

difficulty for their scaffolding in electrospinning and 3D printing.However, the possibility of easily varying the nature of the PPEs pendant side groups via the synthesis process allows for valuable pendant unsaturations to be inserted for their subsequent cross-linking, which will modify their mechanical properties and open up possibilities for their scaffolding[52,53].

1.3.2 PPEs Synthesis

Among the main methods for obtaining PPEs, polycondensation synthesis is probably the most widely used, involving the reaction of a diol with a dialkyl phosphate[39]. This method has the advantage of starting with commercially readily available monomers.

Other methods are also used for the synthesis of PPEs such as the phase transfer catalysis (PTC) method because of its simplicity, low reaction temperature and the linearity of the polymers obtained[54]. There are also methods for synthesizing PPEs by acyclic diene metathesis (ADMET)[39] or using ring-opening metathesis polymerization (ROMP)[55].

However, these different synthesis methods have drawbacks for systems in which the presence of water can lead to side reactions such as hydrolysis of ester bonds or terminal groups of the polymer chain. In addition, synthesis methods such as polycondensation and ADMET require reaction temperatures above 50 C°, reaction times above 10 h for a polydispersity index of the final product above 2[53,56].

Another method of synthesis of PPEs which has the main advantage of better control of the molecular weight and with lower polydispersity index is the ROP (ring-opening polymerization) which is a pseudo-ionic polymerization reaction. A study carried out by B. Clément et al.[57] presents a method of synthesis carried out by pseudo-anionic ROP using non-metallic catalysts with a reaction temperature of 0C°, a reaction time of less than 1h and molar mass as high as 70,000g/mol. In this study, the synthesis is carried out in the presence of benzylic alcohol as initiator and of DBU and TU which are respectively catalysts activating the nucleophilicity of the alcohol and the electrophilicity of the phosphorus (Fig. 8-9). It is a reaction during which an alcohol will act as a nucleophile on an electrophile phosphate located in a ring[52,57-58]. This opens to give rise to an O-terminal anion which will in turn be able to react with another phosphorus.

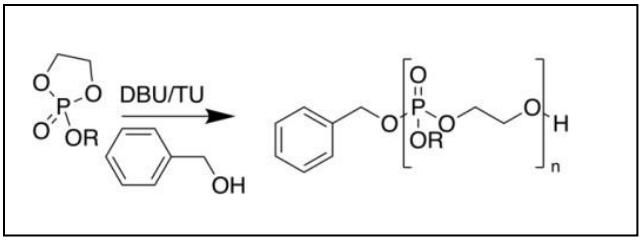

Figure 8: Synthesis of PPEs by ROP[59].

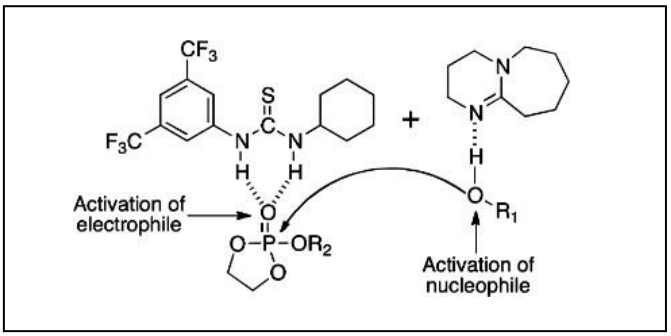

Figure 9: Mechanism of ring-opening polymerization activation for the synthesis of polyphosphoesters in the presence of TU andDBU[57].

2. Objectives & Strategies

Biocompatible and degradable PPEs are promising polymers for biomedical applications, especially in tissue engineering. Depending on the nature of the lateral pendant chain, the chemical properties of the corresponding polymer can be easily adapted for a specific application leading to materials with remarkable physico-chemical properties as described by Riva et al[52] and Rabaux et al[39].However, the networks developed in both researches don't fulfill all the specifications required for a direct application in tissue engineering. Indeed, even though they are able to swell in water, the porosity remains too small for cell penetration, and complex shapesare difficult to reach.

The objective of the master thesis is to determine the experimental conditions toallow the implementation of PPEs by one technique commonly used for the design of tissue engineering scaffolds, namely electrospinning. The main challenge of this research relies on the intrinsic properties of PPEs, which are amorphouselastomers at room temperature and characterized by a glass transition temperature (T_g) around -70°C, which make them not straightforward for electrospinning.

The first step of this research is to determine how the molar mass of PPE and the length of the pendant chains influence the viscosity of the pure statistical copolymer. For this, different statistical copolymers of PPE will be synthesized and characterized by rheology.

The second objective is the fixation of the shape of the nanofibers filaments after electrospinning. Indeed, as mentioned before, PPEs are amorphous elastomers and lose rapidly the targeted shapeby flowing. In order to overcome this issue, a fast photo-crosslinking process of PPEs under UV irradiation just after implementation is mandatory. For this purpose, photoreactive monomers will be statistically incorporated in the PPE backbone, known to allow the cross-linking of PPEs copolymers as described previously.

In order to speed up the cross-linking, methacrylic moieties will also be introduced on both chain-ends. Typically, cyclic phosphate monomer bearing a photoreactive butenyl pendant chain will be copolymerized by ring-opening copolymerization with cyclic phosphate monomer bearing a butyl or a heptyl pendant chain initiated by tetraethylene glycol. Indeed, the length of the non-polar alkyl pendant chain can modify parameters such as the orientation and the mobility of the PPE chains, which significantly influence viscosity and linking density. The impact of the nature of the pendant chain on the viscosity and cross-linking kinetics will be investigated. At the end of the copolymerization, methacrylic moieties will be introduced by reaction of both hydroxyl chain-ends with isocyanate bearing methacrylate (Fig.10).

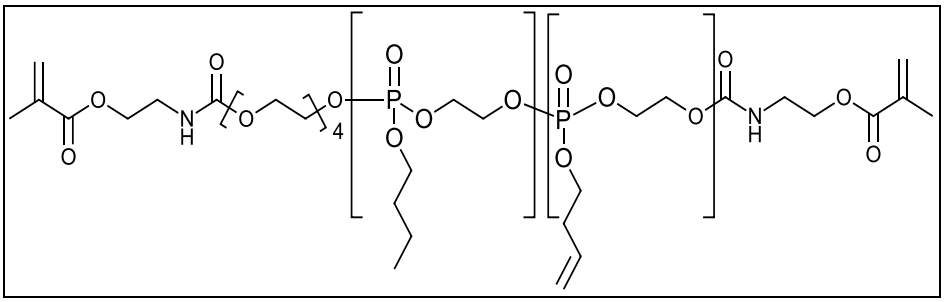

Figure 10: General synthesis of photo-crosslinkable Poly(BenEP-stat-BEP) (BenBP).

Since the time required to reach effective cross-linking is the key parameter to fix the shape of the PPEs after processing, the evolution of the storage and loss moduli during UV irradiation will be followed by rheological measurements. Determining the irradiation time required to reach the gel point will be useful to determine whether the PPE copolymers studied fix quickly enough so that during the electrospinning process, the PPE does not have time to elapse between the moment it is deposited and the moment it is fixed.

Finally, the electrospinning of the most promising PPE copolymers will be carried out under UV irradiation in order to collect and characterize the material obtained.

3. Materials & Methods

3.1 Synthesis and characterization of the monomers and the polymers

3.1.1 Synthesis of monomers

Three varieties of monomers were synthesized from 2-chloro-3-oxo-1,3,2-dioxaphospholane (COP), as illustrated in Figure 11.

In a reaction flask, under anhydrous conditions, a mixture containing 16.2 mL (175 mmol) of n-butanol, 25 mL (180 mmol) of triethylamine, and 175 mL of THF was prepared and cooled in an ice bath. Subsequently, a solution comprising 25g (175 mmol) of COP dissolved in 25 mL of THF was added dropwise to the reaction flask (Fig.12).

Similarly, for the substitution with 1-buten-4-ol and heptanol, there action was conducted under identical conditions and molar ratios.
Specifically, 16.2 mL (175 mmol) of 1-buten-4-ol and 24 mL (175 mmol) of heptanol were employed.

These reactions were performed using flame-dried glassware under an inert atmosphere of nitrogen (N2), with dried THF serving as the solvent. Priorto use, each reactant was dried over CaH2 powder and distilled.

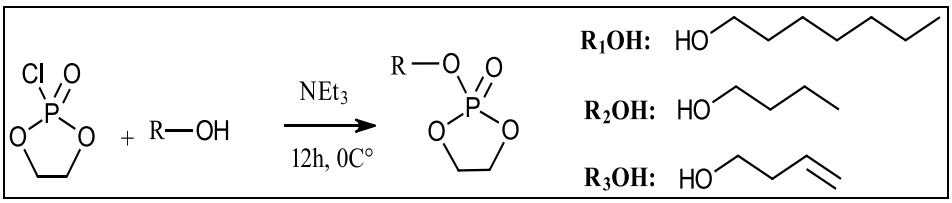

Figure 11: Synthesis of 3 monomers for the synthesis of copolymers statistical polyphosphoesters from COP and primary alcohols.

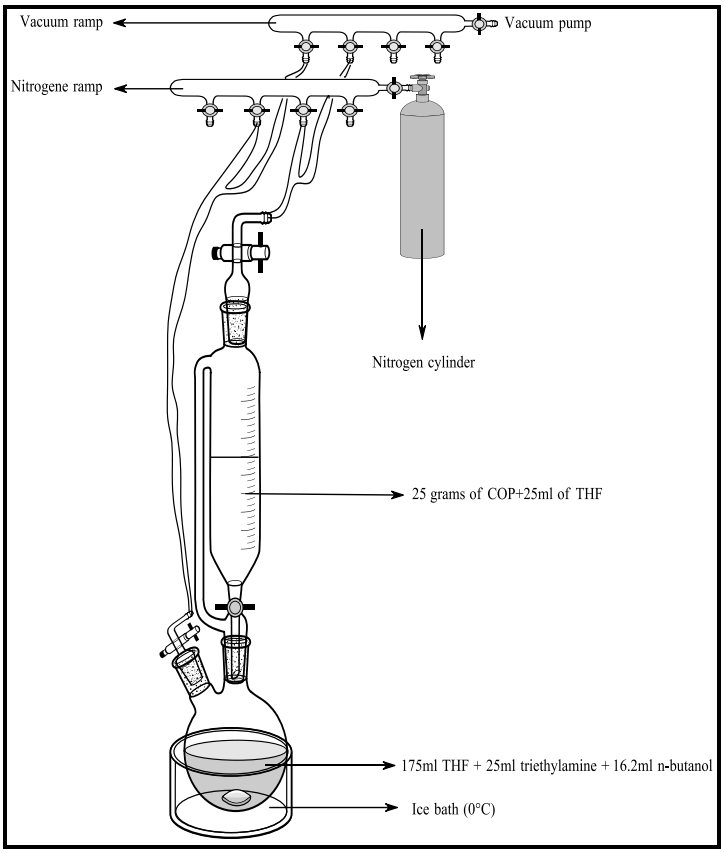

Figure 12: Experimental setup for the synthesis of butyl cyclic phosphate monomer (BP) under anhydrous conditions.

3.1.2 Synthesis of statistic copolymers

The polymerization was an organo-catalyzed ROP using a bifunctional initiator, tetraethylene glycol. The catalyst system was a combination of DBU and TU.

In the first step, TU powder and tetraethylene glycol were added together and dried in an azeotropic mixture with toluene in the reaction flask. Then, the 2 monomers followed by 11 ml of anhydrous dichloromethane were added to the reaction flask. Finally, DBU was added.

After 45 minutes, 2-isocyanatoethyl methacrylate was added and the reaction was allowed to run for 30 minutes. The entire polymerization was carried out at 0 °C.

The monomers were added in stoichiometric amounts. The details for the masses and volumes of reactants and catalysts used for each of the polymers are given in the figure 13.

	BenBP (30,000 g/mol)	BenHP (30,000 g/mol)	BenBP (70,000 g/mol)
BP	4 g		6 g
BenP	4 g	2,67 g	6 g
HP		3,33g	
TU	256 mg	167 mg	317,2 mg
DBU	0,21ml	0,14 ml	0,12 ml
2-isocyanatoethyl methacrylate	0,16 ml	0,1 ml	0,24 ml
Tetraethylene glycol	54 mg	35.1 mg	33,3 mg

Figure 13: Amount of reagent used in mass and volume.

The polymer was then precipitated drop by drop in cold diethyl for BenBP and in heptane for BenHP. The polymer is then left in this solution in the freezer overnight.. Then, the diethyl ether or heptane supernatant was extracted by and the polymer was solubilized in a minimal amount of methanol. It was then dialyzed in methanol twice for two hours using a dialysis membrane (100-500 g/mol). Finally, the methanol was evaporated, and the polymer was dried under vacuum to ensure that all the methanol was removed.

3.1.3 Characterization of the monomers and polymers

a) Gel permeation chromatography

Gel permeation chromatography (GPC) is a size exclusion chromatography where separation is based on macromolecule size and molecular weight. As the sample passes through the column, larger molecules are eluted earlier than smaller molecules. The instrument used to perform GPC analysis is an Agilent 1260 infinity II in THF.

b) Nuclear magnetic resonance

Monomers and polymers were characterized by ^{1}H and ^{31}P NMR in deuterated chloroform. 15 mg of product were dissolved in 700 µL of solvent. 1H and 31P NMR spectra were recorded at 400 MHz in FT mode using a Bruker Avance 400 instrument equilibrated at 25 °C.

c) Scanning electron microscopy:

Samples were sputtered with gold under vacuum and argon flow with an electric current of 30 mA. Images were recorded with a Philips XL30 FEI ESEM in Secondary Electron mode. Images were then analyzed with ImageJ software.

d) Differential scanning calorimetry

Differential scanning calorimetry (DSC) is a method that enables the determination of the transition temperatures of the polymers and the associated heat flow. The sample and an intern reference are heated following a specific temperature program. DSC measures the amount of heat produced to keep constant the temperatures of both the sample and the reference. The instrument used was a TA Instrument Q100. The program used first started by a cooling down phase until -80°C followed by a ramp of temperature of 10°C/min up to 100°C.

e) Fourier Transformed InfraRed Attenuated Totally Reflected Spectroscopy (FTIR-ATR)

A Thermo Scientific iD5 FTIR-ATR spectrometer was used to analyze the chemical composition at the surface of the precursors and materials.

3.2 Rheological analyses

Rheology is the study of the mechanical properties of fluid and solid materials by observing the response of the material studied under mechanical stress. Experimental measurements in rheological science can be carried out in different ways.For a viscosity measurement, we find the classic methods of using capillary viscometers or the Stokes method. To find out about parameters linked to mechanical properties such as the Young's modulus, there are the classic tension and compressiontests**.** A slightly more modern technique that allows data to be obtained on the viscosityand strain measurements of a material is the use of what is called a rheometer. This works as shown in Figure 14.

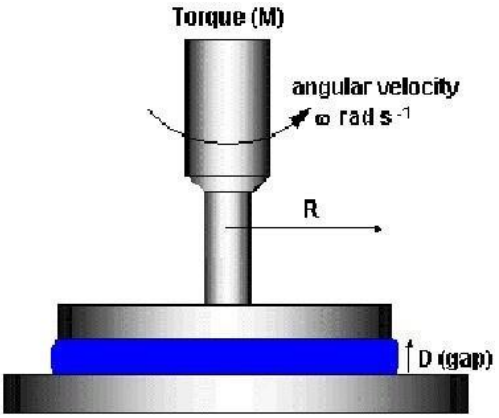

Figure 14: Principle of rheometer with parallel plate system[60].

The analytical substance is placed between 2 metal devices, a stator located below the substance and a rotor located above. The strain is transmitted to the substancevia the rotor and the response of the substance is analyzed via a specific data processing computer system. The geometry of the stator and rotor varies depending on the substance to be analyzed, the substance can be placed between two parallel plates if itis viscous enough, the concentric cylinder geometry also exists for less viscous substances with the outer surface for the stator and an inner cylinder for the rotor.

In the context of the rheological study of polymers, it is important to indicate that they can be described by a combination of both elastic behavior where the polymerwill tend to store strain energy and viscous behavior where the polymer will tend to lose this strain energy. This combination of these two behaviors is called viscoelastic behavior.

In the same way that it is possible to describe these two behaviors by stress-strain relationships, the viscoelastic behavior can be described according to the Maxwel model by adding the elastic and viscous component in the expression of the applied stress. Thus, for a viscoelastic behavior we have that:

$$\sigma\ total = E.\varepsilon\ +\ \eta.\frac{dS}{dt} \qquad (2)$$

With σ is the applied stress in Pa, the deformation induced on the polymer ε in %, E,the modulus of elasticity in Pa and the viscosity η in Pa.s.

From eq.2, we deduce that[61]:

$$\sigma\ total = \varepsilon(0).(E.\sin(\omega t)\ +\ \eta.\omega\ \cos(\omega t)) \quad (3)$$

Assuming that G'=E and G"= $\eta.\omega$ with ω the rotation frequency of the rotor,we have the following final equation:

$$\sigma\ total = \varepsilon(0).(G'(\omega).\sin(\omega t)\ +\ G''(\omega)\cos(\omega t) \quad (4)$$

With G' the storage module and G" the loss module. The intensity of the elastic and viscous components of a polymer can be determined with a rheometer via the determination of G' and G".

In my studies, rheology was performed for the determination of the gel point under UV irradiation of the polymers and for the measurement of viscosity.

The gel point is, as its name suggests, the point where the loss modulus and the modulus of elasticity are such that the polymer studied is sufficiently cross-linked to form a solid polymer which, for example, in the presence of water, can create a hydrogel. The gel point is reached when the storage modulus G' and the loss modulus G" intersect.

The plate/plate geometry is chosen when the polymer is sufficiently viscous at the start. The sample is placed on the lower plate and the final gap between the 2 plates is reached when the sample forms a "buoy", i.e. the circular edge of the sample protrudes outwards. As soon as the sample is placed under UV light, the gel point measurement begins.

To measure viscosity with a rheometer, you can either maintain a constant shear stress or gradually increase the frequency of the shear stress. The second method is particularly interesting because it allows the observation of a phenomenon called shear thickening, where the material becomes thicker under certain conditions. There is also the opposite effect, shear thinning where the material becomes less viscous. These phenomena are important in the context of electrospinning, because during the spinning process, the polymer is subjected to stresses that can affect its properties.

Polymer viscosities and gel points were recorded in a frequency sweep experiment at 1% strain with a fixed given temperature. Polymers were prepared with 5 wt% photoinitiator I2959 and then tested on the ARES G2 rotational rheometer (TA instruments) at 1 Hz frequency and 1% strain.

3.3 Electrospinning

A solution of 2 g of pure polymer with a few drops of methanol is mixed for 1 hour with 5% by weight of Igracure 2959 as a photoinitiator. The prepared solution was loaded into a masked syringe with opaque blue tape to block exposure to light during the electrospinning process. This solution is electrospun for 1 hour on a sheet of aluminum foil with a flow rate of the solution that is set at 13 µL/min. A potential of 12kV is applied once the solution is visible at the tip of the needle, creating a fluid jet. At this point, the light source was turned on to cure the polymer fluid jet. The light was positioned about 15 cm from the fiber and directed towards the collector.

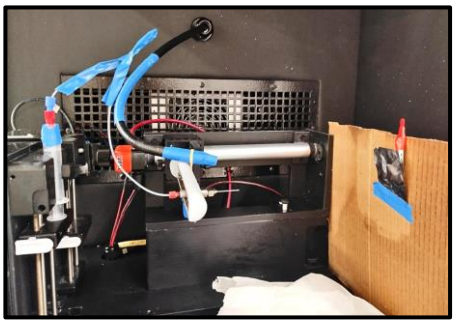

Figure 15: Electrospinning setup under UV irradiation.

4. Results & Discussion

4.1 Synthesis of PPE copolymers bearing unsaturations

PPEs have to be processed by electrospinning and therefore, a high molar mass has to be targeted to allow chain entanglement. In addition, the PPEs have to be photocrosslinkable in order to fix the fiber morphology during electrospinning. Therefore, we decided to introduce some unsaturations as side-chain along the backbone so as an acrylic group at the chain-end to enable the further cross-linking. The synthesis of random copolymers of butenyl cyclic phosphate monomer (BenP) with either butyl cyclophosphate (BP) or heptyl cyclophosphate (HP) by organocatalyzed ring-opening copolymerization was targeted since this chain growth mechanism allows control of the molar mass and relatively high polymerization degrees can be targeted. A difunctional initiator has been selected leading to hydroxy- telechelic copolymers whose both chain-ends can be functionalized further to bear an acrylic moiety. The structure of the targeted functional copolymers BenBP is given in Figure 10. For BenHP, the pendant butyl chain is replaced by a heptyl chain.

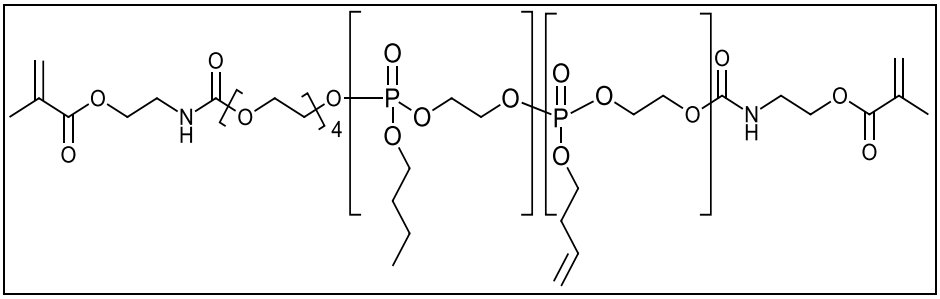

Figure 10: General synthesis of photo-crosslinkable Poly(BenEP-stat-BEP) (BenBP).

The copolymers were characterized using ^{1}H and ^{31}P NMR, as well as GPC and DSC. Firstly, 1H NMR was employed to assign the signals corresponding to the protons of the pendant chains and the initiator. For 31P NMR, the chemical shift of phosphorus in the polymer backbone was observed at approximately 0.5 ppm, while the phosphorus signal of the unreacted monomer appeared near 17 ppm. This distinction highlights the utility of 31P NMR in confirming the successful polymerization and ensuring that all the monomer was consumed.

Following the synthesis of BenBP, Figure 17 provides clear and direct visual confirmation that polymer has been formed. ^{31}P NMR before dialysis of the synthesized copolymer allows easy verification if there is any monomer left.

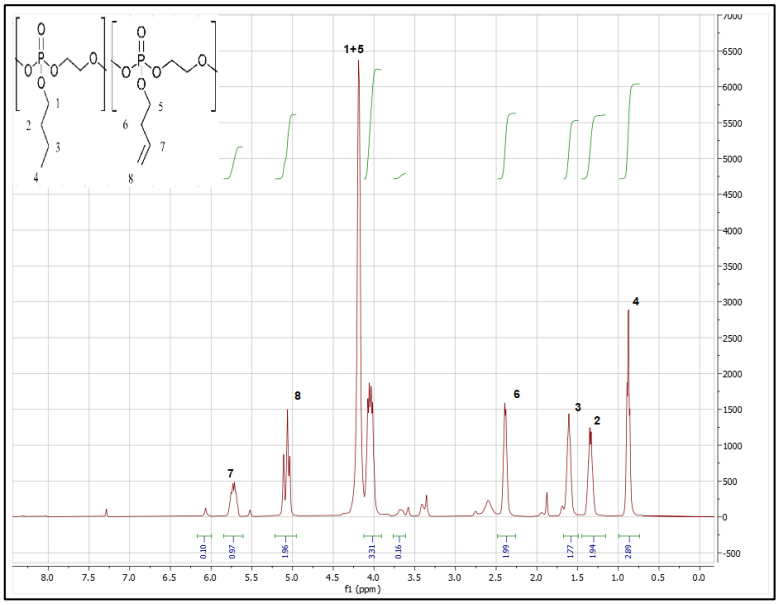

Figure 16: NMR ^{1}H polymer BenBP spectrum (25,954 g/mol).

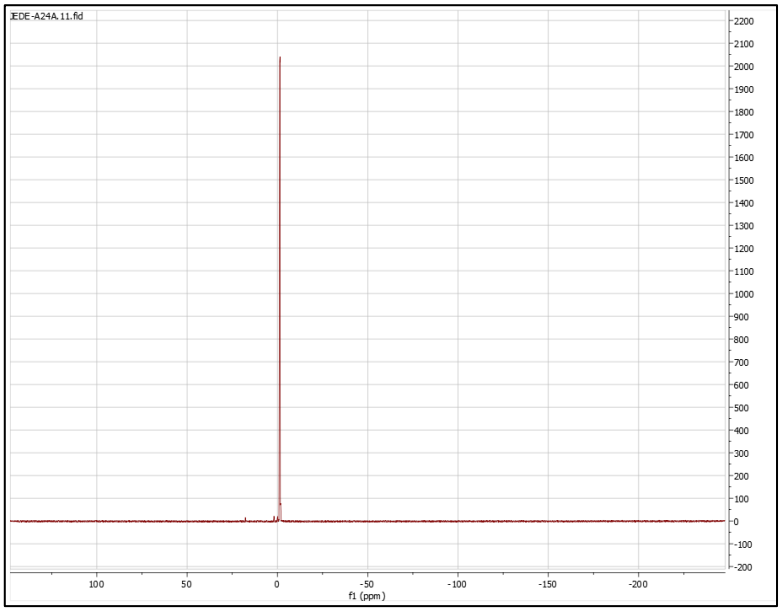

Figure 17: NMR ^{31}P polymer BenBP spectrum(25,954 g/mol).

The values below show the chemical shifts of the proton of the pendant chains and the initiator:

Proton number (Fig.16)	chemical displacement (ppm)	Integration
Proton 4 (3 protons)	0.9	2,89
Proton 2 (2 protons)	1,4	1,94
Proton 3 (2 protons)	1,6	1,77
Proton 6 (2protons)	2,4	1,99
Proton primer (12 protons)	3,7 and 3,64	0,16
Proton 1+5 (4 protons)	4,1	3,31
Proton 8 (2 protons)	5,2	1,96
Proton 7 (1proton)	5,8	0,97
Proton methacrylate (2 proton)	6,06	0,1

Figure 18: Chemical shift values and proton integrations of the NMR spectrum of the BenBP polymer in figure 16.

The chemical shift of vinyl protons of methacrylate was determined by comparing the spectrum before addition of methacrylate and after addition of methacrylate. Only these protons of methacrylate are visible.

The calculation of the experimental molar mass was carried out using the following formula:

$$Molar\ mass\ BenBP = \left(\frac{\int proton\ 7}{\int proton\ primer} \times molar\ masse\ BenP\right) + \left(\frac{\int proton\ 4}{\int proton\ primer} \times molar\ masse\ BP\right)$$

Each integration takes the values reduced to 1 single proton, so we obtain:

$$Molar\ mass\ BenBP = \left(\frac{0{,}97}{0{,}16/12} \times 178\right) + \left(\frac{2{,}89/3}{0{,}16/12} \times 180\right) = 25954\ g/mol$$

The ratio of BEP and BenEP in the polymer chain was determined with the following formulas:

$$Percentage\ of\ BenEP = \frac{\int proton\ 7}{\int proton\ 7 + \int proton\ 4} \times 100$$

$$Percentage\ of\ BEP = \frac{\int proton\ 4}{\int proton\ 7 + \int proton\ 4} \times 100$$

In this way we obtain:

$$Percentage\ of\ BenEP = \frac{0{,}97}{0{,}97 + (\frac{2{,}89}{3})} \times 100 = 50{,}17\%$$

$$Percentage\ of\ BEP = \frac{2{,}89/3}{0{,}97 + (\frac{2{,}89}{3})} \times 100 = 49{,}83\%$$

The exact amounts of reagent and catalysts to add for the synthesis are shown in the figure 19.

Reagent	**Theorical mass**	**Experimental mass**
BP	4 g	4,098 g
BenP	4 g	4,1624 g
TU	256 mg	271 mg
DBU	0,21 ml	0,21 ml
Primer	54 mg	49 mg
methacrylate	0,16 ml	0,2 ml

Figure 19: Theoretical and actual amount of reagent added for the synthesis of BenBP (25,954 g/mol).

The exact added mass of BP monomers is 4.098 g and the exact mass of BenP is 4.1624 g, which explains the difference in percentages of BEP and BenEP into the polymer chain.

Considering the exact masses added of monomers and initiator for polymer synthesis, we should obtain a DP of 183. Taking into account the percentages of BEP and BenEP on a chain of 183 monomers, we obtain a theoretical molar mass at 100% conversion of 32,756 g/mol.

The experimental molar mass obtained which is 25,954 g/mol is lower than the value of 32,756 g/mol.. Based on the GPC analysis (Fig.20), we observe that the polydispersity index is 1.238, which supports the hypothesis that this could be attributed to intramolecular transesterification side reactions. The decrease in molar mass is also linked to an incomplete conversion of the monomer into polymer. Indeed, the mass of polymer obtained is 3.0545 g and the mass of monomer used is 8.2604 g. This gives a mass yield

of 37 %.

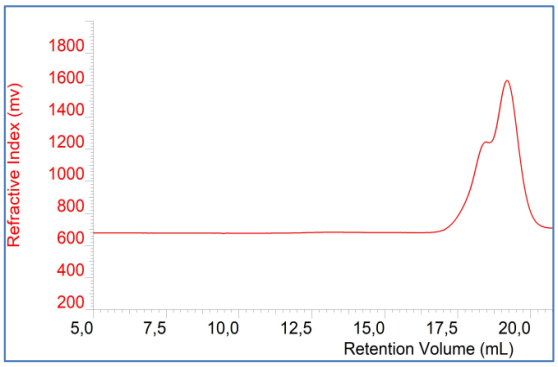

Figure 20: GPC of polymer BenBP (25,954 g/mol).

With the same reasoning as for BenBP, we obtain an experimental molar mass for BenHP of 26,121 g/mol. The percentage of HEP in the chain is 50,35%. the percentage of BenEP is 49,65%. Based on the masses of the reagents actually added, the calculated DP is approximately 160 when rounded. Considering the percentages of BEP and HEP in the polymer chain, the theoretical molar mass of the polymer at 100% conversion is 32,025 g/mol. However, this target value is significantly higher than the experimentale molar mass obtained, which is 26,121 g/mol. According to the GPC analysis (Fig.23), the polydispersity index is very close to 1 (DP=1.101). Consequently, this decrease in molar mass cannot only be attributed to secondary transesterification reactions. This is explained by an incomplete conversion of the monomers. Indeed, the mass of polymer obtained is 3.334 g and the mass of monomer used is 6.0046 g. This gives a mass yield of 56 %.

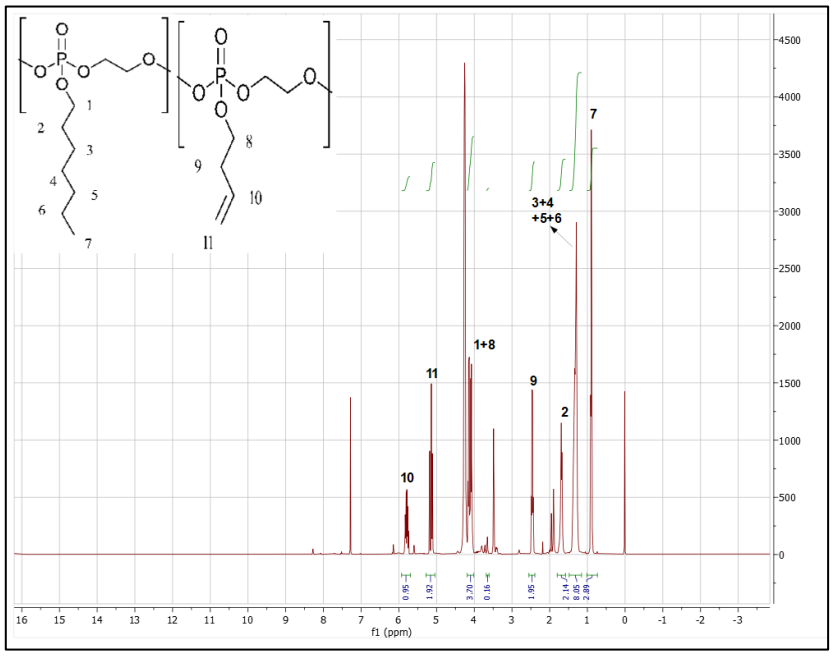

Figure 21: NMR ^{1}H polymer BenHP spectrum (26,121 g/mol).

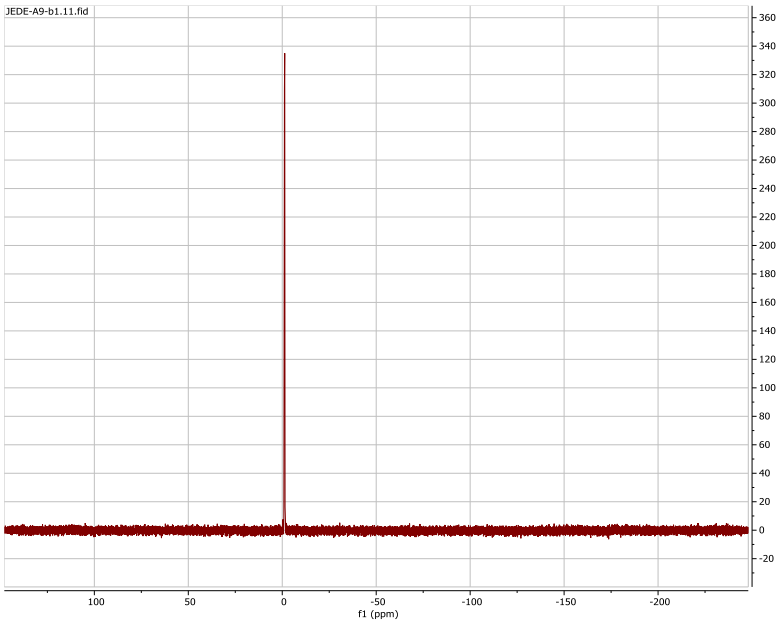

Figure 22: NMR ^{31}P polymer BenHP spectrum(26,121 g/mol).

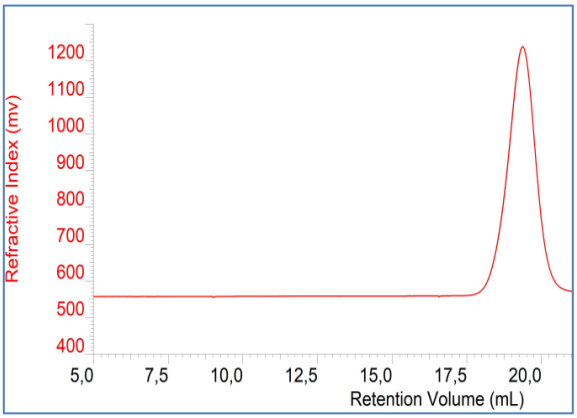

Figure 23: GPC of polymer BenHP (26,121 g/mol).

For the BenBP polymer of higher molar mass we obtain an experimental molar mass of 74,432 g/mol. The percentage of BEP in the chain is 46.15%. The percentage of BenEP is 53.85%. Based on the masses of the reagents actually added, the calculated DP is 382. Considering the percentages of BEP and HEP in the polymer chain, the theoretical molar mass of the polymer at 100% conversion is 68,349 g/mol. The experimentale molar mass obtained which is 74,432 g/mol is higher than the value of 68,349 g/mol.. Based on the GPC analysis (Fig.26), we observe that the polydispersity index is 1.791, which supports the hypothesis that this could be attributed to intermolecular transesterification side reactions. The mass of polymer obtained is 7.6697g and the mass of monomer used is 12.0241 g. This gives a mass yield of 64 %.

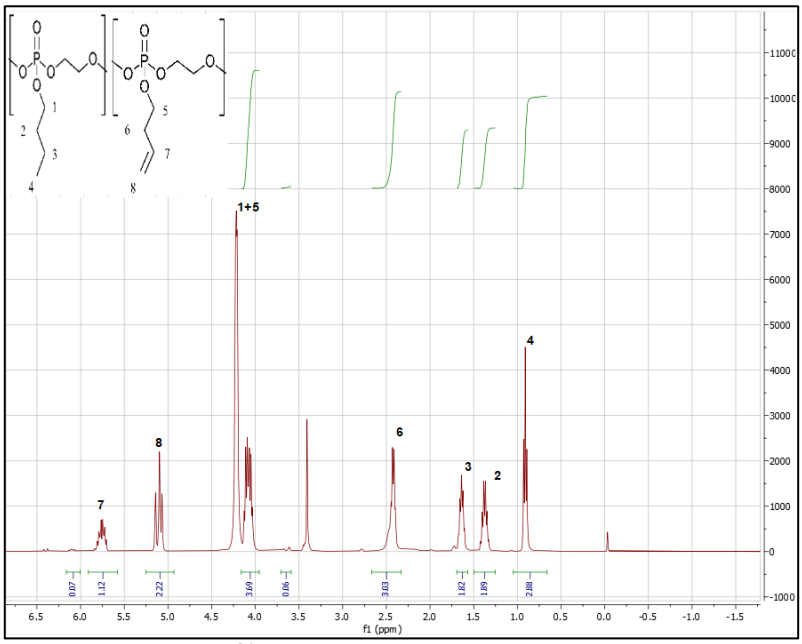

Figure 24: NMR ^{31}P polymer BenBP spectrum (74,432 g/mol).

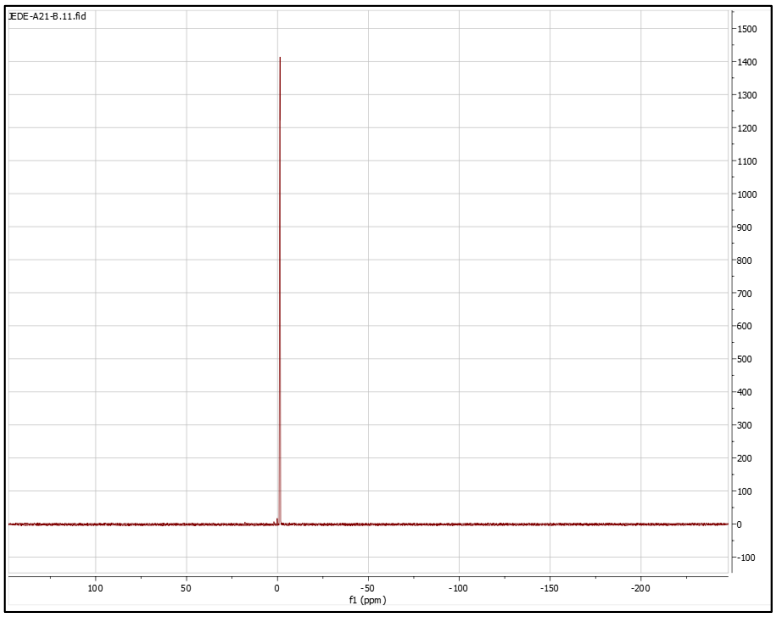

Figure 25: NMR ^{31}P polymer BenBP spectrum (74,432 g/mol).

GPC analysis (Fig. 26) revealed a polydispersity index (PDI) of 1.791. This relatively high value can be attributed to the findings of Clement et al.[57], who explain that the synthesis of PPEs via ring-opening polymerization is inherently limited to molar masses below 70,000 g/mol. Beyond this threshold, transesterification reactions become

predominant, leading to broader molecular weight distributions.

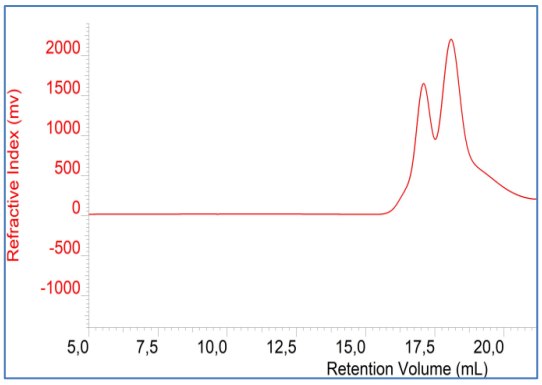

Figure 26: GPC of polymer BenBP (74,432 g/mol).

The glass transition temperatures were also determined by DSC for each of these 3 PPEs. The Tg for BenHP (26,121 g/mol), BenBP (26,843 g/mol) and BenBP (74,432g/mol) are respectively -60,49C°,-69,78C° and -72,61C°.

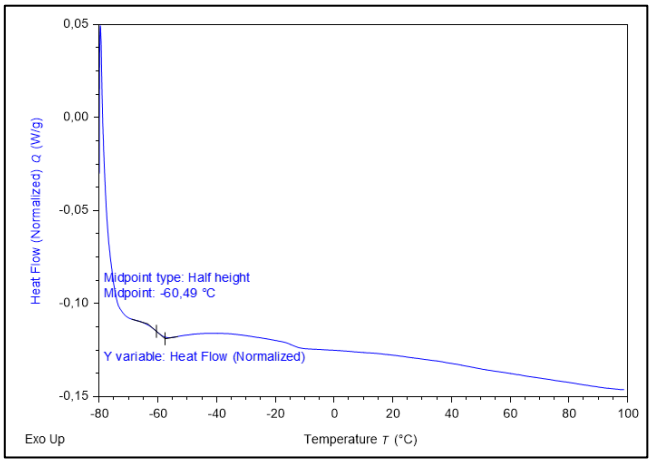

Figure 27: DSC of polymer BenHP (26,121 g/mol).

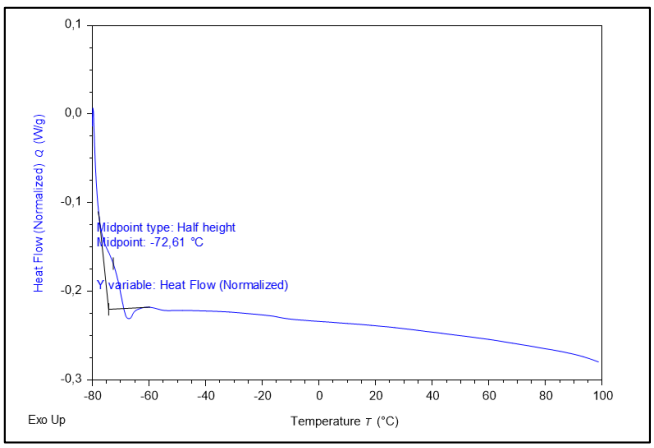

Figure 28: DSC of polymer BenBP (74,432 g/mol).

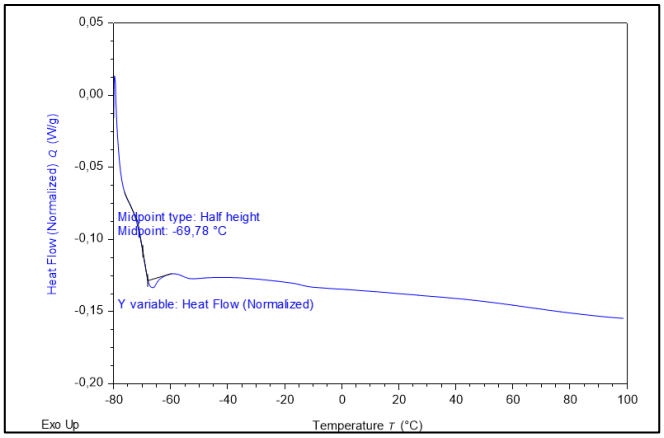

Figure 29: DSC of polymer BenBP (26,843 g/mol).

Tg is much lower than room temperature, so the amorphous PPEs we are working on are liquid at room temperature. Therefore, during the electrospinning process, once the PPE is deposited on the collector, it will flow directly and it is then impossible to obtain fixed nanofibers. The strategy for fixing the PPEs once deposited on the collector is explained in the following section

4.2 Results of cross-linking kinetics

In this work, the strategy to stabilize the nanofibers involves directing a UV light source at the collector during the electrospinning process. This approach enables the PPE to cross-link via its photoactive chains, preventing the chains to flow on the collector.

To successfully obtain fixed nanofibers, the cross-linking rate must be sufficiently fast to prevent the PPE from flowing before it solidifies. To evaluate this, the cross-linking speed was measured by determining the time required to reach the gel point of PPE under UV irradiation. Measurements were conducted both without an initiator and with 5 wt% of the photoinitiator IG2959.

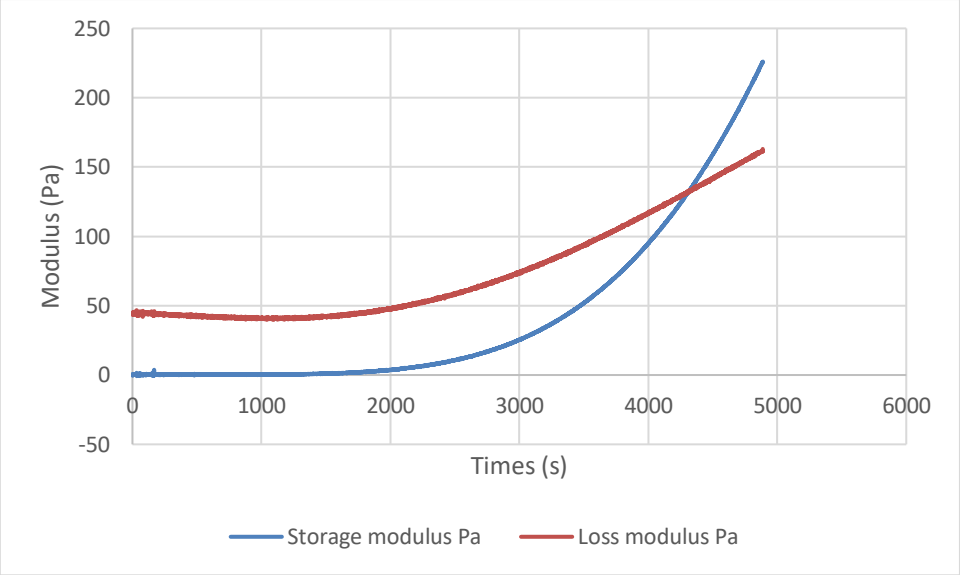

Figure 30: Rheometer measurement of the gel point of the statistical copolymer BenBP without initiator. It takes 1 hour and 12 minutes (4312 seconds) to reach the gel point.

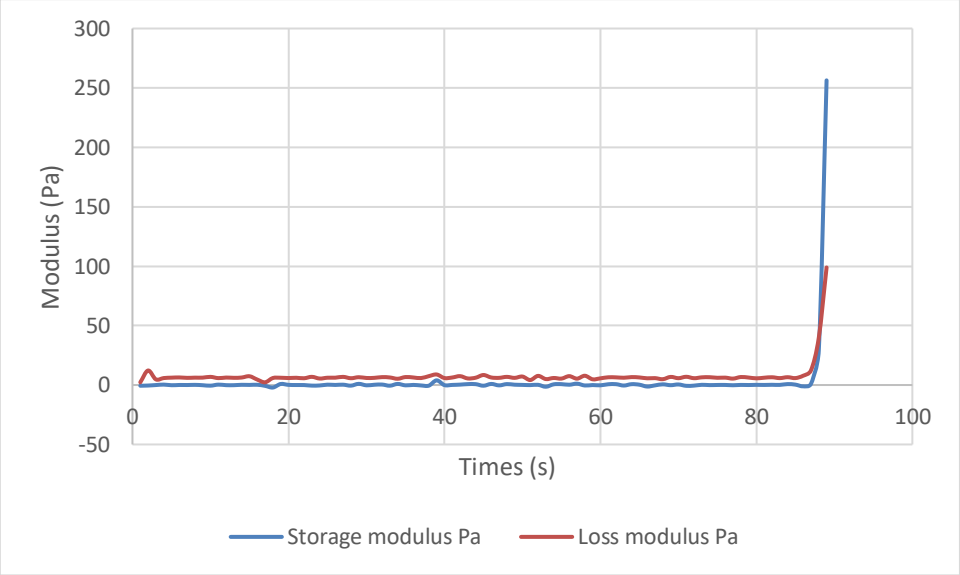

Figure 31: Rheometer measurement of the gel point of the statistical copolymer BenBP with 5% of initiator. It takes 1 minutes and 29 secondes to reach the gel point.

It is observed that the photo-crosslinking rate is higher in the presence of an initiator than in its complete absence. In the presence of the initiator, the gel point is achieved in 1 minute and 29 seconds. However, this time suggests that the polymer has sufficient opportunity to flow between deposition on the collector and complete solidification. Moreover, during the rheology measurements, UV light is precisely focused on the sample using a mirror, providing an idealized scenario. Under the actual conditions of

electrospinning, it is anticipated that the time required to reach the gel point may be longer.

To address this issue and prevent the polymer from flowing between deposition and solidification, the proposed strategy is to cool the collector below the Tg of the amorphous PPEs using dry ice (-78°C). Electrospinning tests will be conducted with both a room-temperature collector and a collector cooled to -78°C to evaluate the effectiveness of this approach.

Before proceeding with electrospinning tests, it is crucial to verify that the PPEs exhibit suitable viscosity for spinning. This aspect will be addressed in the following section.

4.3 Determination of PPE solution viscosity

As discussed in Section 1.2, a polymer solution becomes electrospinnable beyond the entanglement concentration, up to an upper viscosity limit where the solution becomes too viscous to process. Electrospinnable solutions generally exhibit viscosities in the range of 0.01 Pa·s to 100 Pa·s, as reported in previous studies[21-22,25].

To establish a reference point, a viscosity test was conducted on an electrospinnable solution 2.10^{-3} M of polycaprolactone (Mw = 80,000 g/mol) in DMF and THF as solvents (Fig. 32).

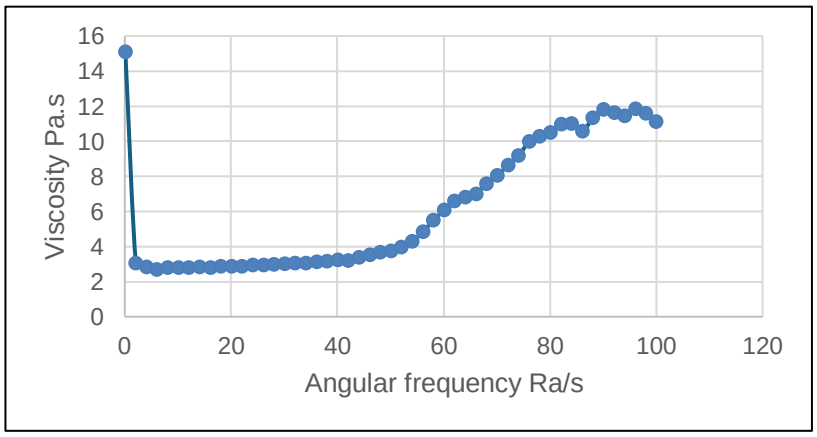

Figure 32: Rheometer measurement of the complex viscosity of an electrospinnable solution of polycaprolactone. Average of the measurement: 2.95 Pa.s.

The measured viscosity was 2.95 Pa.s. Viscosities were determined as the average

complex viscosity over an angular frequency range where viscosity variation was minimal. A frequency sweep was applied to all viscosity measurements to identify any rheo-thickening or rheo-fluidifying behavior. In Figure 32, a sudden increase in viscosity beyond 40 rad/s was observed. PCL is a semi-crystalline polymer with a melting temperature of 60°C. Consequently, once all the solvent has evaporated, the PCL rapidly solidifies at room temperature. This abrupt increase in viscosity is therefore attributed to the rapid evaporation of the solvent rather than a rheo-thickening effect.

Viscosity ranges of less than 10 Pa.s and between 40 Pa.s and 100 Pa.s appear to correspond to electrospinnable solutions. Additionally, polymer solutions with concentrations between 10% and 30% by mass and molar masses from tens of thousands to several hundred thousand g/mol can also be electrospinnable.

Based on these findings, rather than determining the entanglement concentration of various PPEs solutions initially, preliminary viscosity tests were conducted on 100% PPE solutions to estimate the appropriate concentration range for direct electrospinning tests. The two PPEs tested were BenBP and BenHP, each with an approximate molar mass of 20,000 g/mol.

As outlined in Section 1.2.2, according to Mark-Houwink's relationship, higher molar mass correlates with increased viscosity. For electrospinning, a polymer with excessive viscosity is preferable to one with insufficient viscosity, as it can be diluted with an appropriate solvent or solvent mixture. Given the importance of solvent evaporation during the spinning process, a higher molar mass BenBP polymer (~70,000 g/mol) was synthesized, and its viscosity was measured.

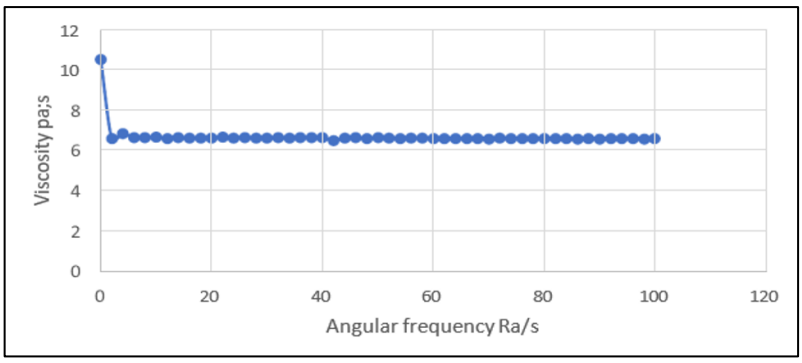

Figure 33 : Rheometer measurement of the complex viscosity of the statistical copolymer BenBP (22,600 g/mol) 100% previously dried empty. Average of the measurement: 6.65 Pa.s.

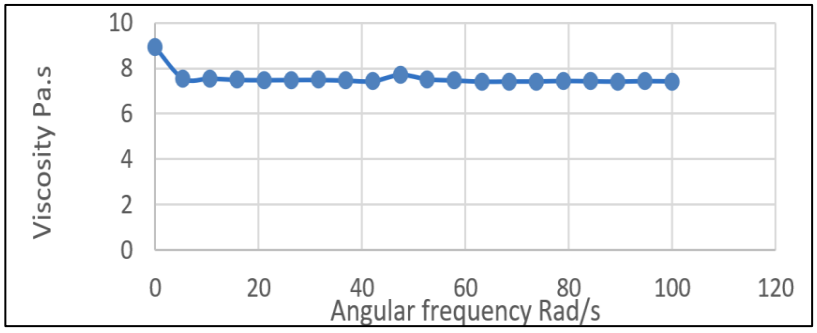

Figure 34 : Rheometer measurement of the complex viscosity of the statistical copolymer BenBP (~70,000 g/mol) 100% previously dried empty. Average of the measurement: 7.86 Pa.s.

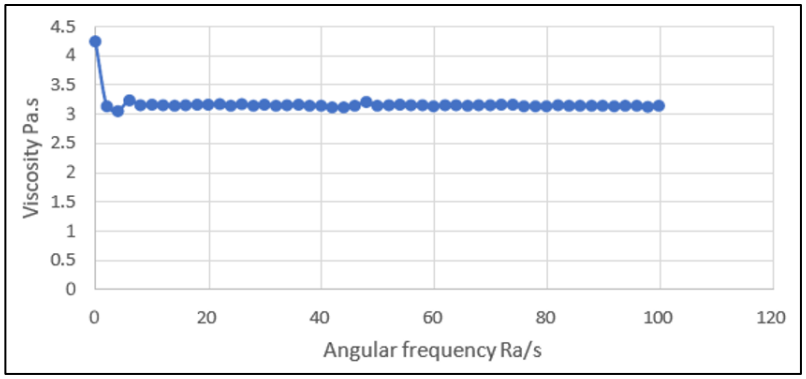

Figure 35 : Rheometer measurement of the complex viscosity of the statistical copolymer BenHP (22,069 g/mol) 100% previously dried empty.: Average of the measurement 3.14 Pa.s.

For the vacuum-dried BenBP copolymer (Mm = 22,600 g/mol), the complex viscosity was 6.65 Pa·s, whereas for the vacuum-dried BenHP copolymer (Mm = 22,069 g/mol), the complex viscosity was 3.14 Pa·s.

The first observation is that the viscosity of BenHP is lower than that of BenBP. This is likely due internal plastification effect due to the longer heptyl pendant chains occupy more space, hindering chain-to-chain interactions and reducing the polymer viscosity.

A second observation is that despite very similar Tg measured by DSC, the viscosity of the BenBP polymer increases significantly (by 1.21 Pa·s) by increasing the molar mass from 22,600 g/mol to 70,000g/mol. This increase reflects a higher molar mass. No sudden increases or decreases in viscosity were observed, confirming the absence of rheo-thickening or rheo-fluidifying effects.

The 100% polymer solutions fall within a viscosity range that could hypothetically correspond to an electrospinnable solution. Therefore, the initial electrospinning tests were conducted on solvent-free PPE solutions. The first electrospinning tests were therefore carried out on solvent-free PPE solutions.

4.4 Electrospinning test

To summarize the findings from the previous sections, the results of Sections 4.1, 4.2, and 4.3 provided the necessary foundation for the electrospinning tests. Section 4.1 demonstrated that BenBP and BenHP were successfully synthesized with a relatively low polydispersity index (PDI) of 1. BenBP (70,000 g/mol) was also synthesized successfully but exhibited a higher PDI.

Section 4.2 revealed a higher cross-linking speed for BenBP in the presence of 5 wt% Irgacure 2959 initiator. However, this cross-linking speed was still insufficient to prevent polymer flow between deposition on the collector and fixation during the electrospinning process. As a solution, the collector will be cooled below the Tg of the polymer using dry ice (-78°C) to stabilize the polymer during photocuring.

Section 4.3 evaluated the viscosities of solvent-free polymers. All three polymers exhibited viscosities within a range hypothetically suitable for electrospinning. BenHP showed a lower viscosity compared to BenBP, this is likely due internal plastification effect due to the longer heptyl pendant chains. BenBP (70,000 g/mol) exhibited a slightly higher viscosity than BenBP (22,600 g/mol). Based on these findings, electrospinning tests primarily focused on BenBP (20,000 to 30,000 g/mol). Some tests were also performed with BenHP (20,000 to 30,000 g/mol) and BenBP (70,000 g/mol) with the collector at room temperature in order to evaluate the spinning process on these polymers. Detailed parameters for electrospinning, solution preparation, and setup are described in Section 3.3.

The electrospinning tests were conducted in two main steps. During the first step, each of the three polymers successfully formed a thread at the needle tip, with the characteristic Taylor cone visible to the naked eye. This confirmed the initiation of the spinning process. However, the threads were only visible in the region near the needle, suggesting that the viscosity and chain entanglement might not be sufficient to sustain thread formation over a longer distance.

Additionally, an electrospinning test was carried out with each of the 3 PPEs with 10

wt% THF without prior viscosity measurements. In this case, no thread was observed; instead, the solution dripped directly from the needle. This behavior suggests that the solution lacked the necessary viscosity for successful electrospinning. Given the already very low concentration of solvent, electrospinning tests in the presence of solvent were abandoned.

The second step involved verifying whether the PPE was deposited on the collector and assessing whether cross-linking occurred, resulting in nanofiber formation. Infrared spectroscopy was used to confirm the presence of PPE on the aluminum foil. A representative IR spectrum was obtained for BenBP deposited on a collector cooled to -78°C (Fig.36). The spectrum of the deposited polymer (blue) was compared to that of non-crosslinked BenBuP (red).

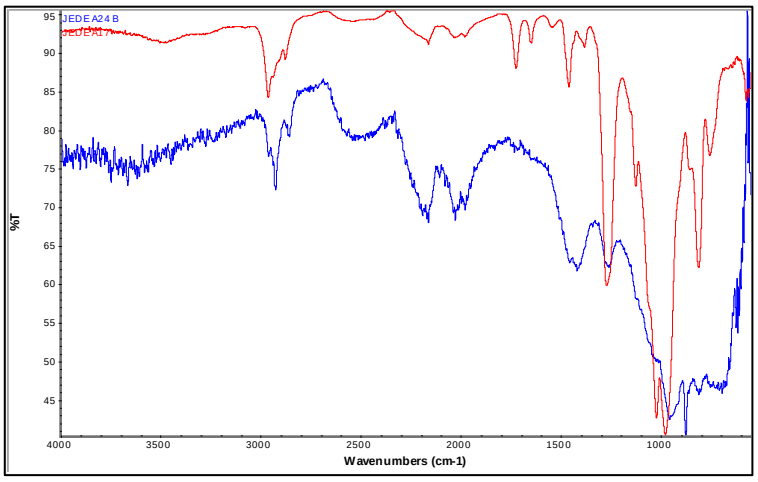

Figure 36 : Infrared spectroscopy of the deposit on the aluminum collector (blue spectrum) and of the reference BenBP (red spectrum).

First of all, we notice that the intense peaks around 1000 cm^{-1} and the average peaks around 3000 cm^{-1} are present on the blue spectrum. We can also observe that the characteristic peaks of the double bonds of the butenyl pendant chains located at 1641 cm^{-1} have completely disappeared.

These observations indicate that PPE was indeed deposited on the aluminum and that it was completely cross-linked. Then, the aluminum sheet alone and the aluminum sheets after electrospinning were observed by optical microscopy and scanning electron microscopy in order to clearly distinguish the intrinsic structures of the aluminum sheet.

4.4.1 BenBP and BenHP solvent-free with ambient temperature collector

Test with solvent-free BenBP (20,000 to 30,000 g/mol): Formation of a wire and deposit on the collector but scanning electron microscopy showed no nanofibers. Figures 37 and 38 show the images of aluminum with deposit after electrospinning.

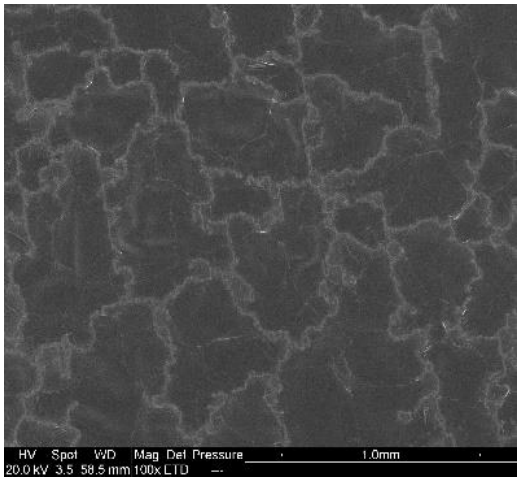

Figure 37: Image of aluminum foil with deposit in scanning electron microscopy (100×).

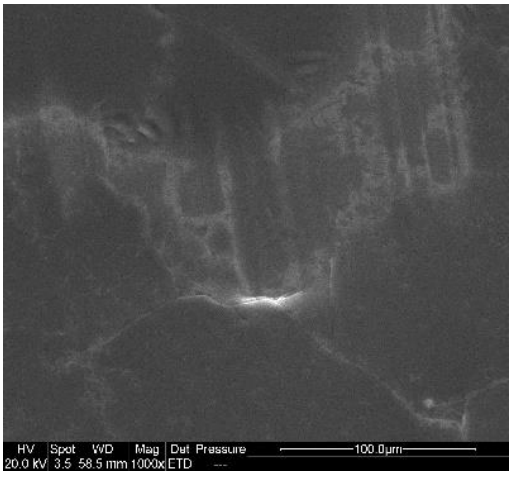

Figure 38: Image of aluminum foil with deposit in scanning electron microscopy (1000×).

The solvent-free test with BenHP (20,000 to 30,000 g/mol) and BenBP (70,000g/mol) gave the same results in electrospinning as for BenBuP (20,000 to 30,000 g/mol), there is formation of a thread at the exit of the needle but the scanning microscopy did not show any deposit of nanofiber.

4.4.2 BenBP (20,000 to 30,000 g/mol) solvent-free with a collector at -78C°

The same basic setup was used for the electrospinning test, but this time the collector was cooled to -78 °C. The dispersed dry ice was wrapped in aluminum foil and then crushed against a flat surface. The resulting horizontal surface is the surface on which the electrospun polymer was deposited. Before performing an electrospinning test, a small amount of PPEs was deposited on a small aluminum foil cooled to -78 °C to check whether the polymer solidifies quickly. This test showed that the PPEs solidifies instantly upon contact with the cooled collector.

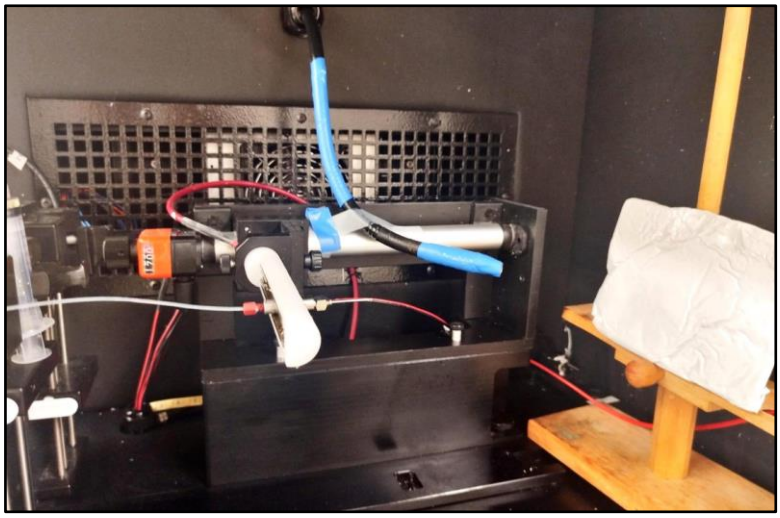

Figure 39: Setup for the electrospinning experiment with a collector cooled with dry ice.

The aluminum foil was then analyzed under an optical microscope in 4×. Figure 40 and 41 show aluminum foil with deposit and Figure 42 and 43 show aluminum foil alone.

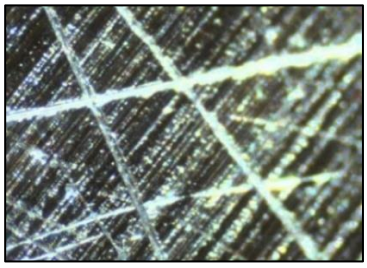

Figure 40: Image of aluminum foil with deposit in optical microscopy [640×480] µm(4×).

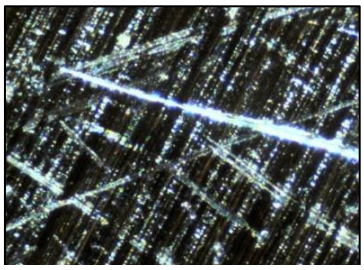

Figure 41: Image of aluminum foil with deposit in optical microscopy [640×480] µm (4×).

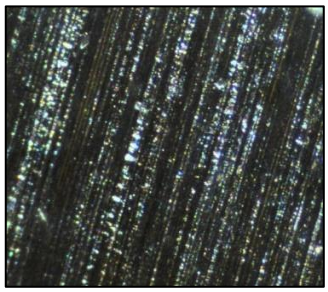

Figure 42: Images of aluminum sheet in optical microscopy [640×480] µm (4×).

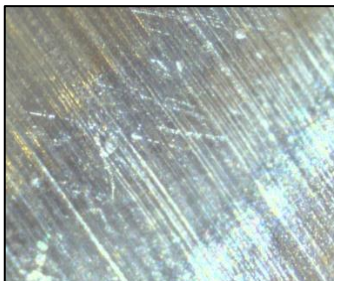

Figure 43: Images of aluminum sheet in optical microscopy [640×480] µm (4×).

Aluminum foils without deposit (Figure 44 and 45) and with deposit (Figure 46 and 47) were also observed by scanning electron microscopy in 250 × and in 1000 ×:

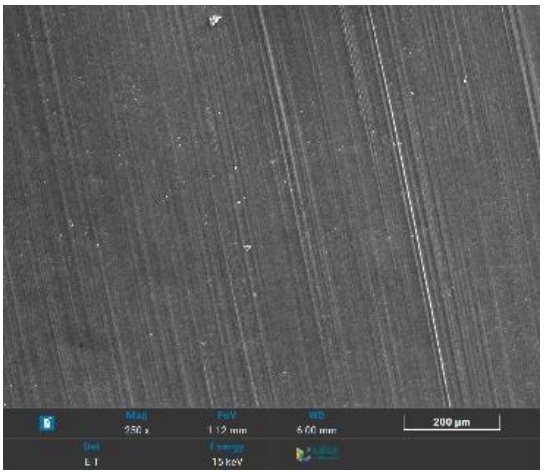

Figure 44: Image of aluminum foil without deposit in scanning electron microscopy (250×).

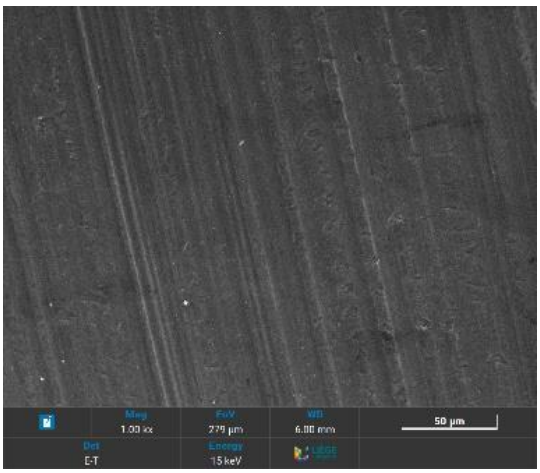

Figure 45: Image of aluminum foil without deposit in scanning electron microscopy (1000×).

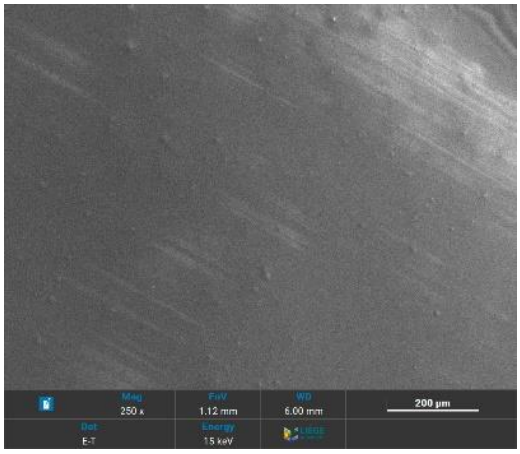

Figure 46: Image of aluminum foil with deposit in scanning electron microscopy (250×).

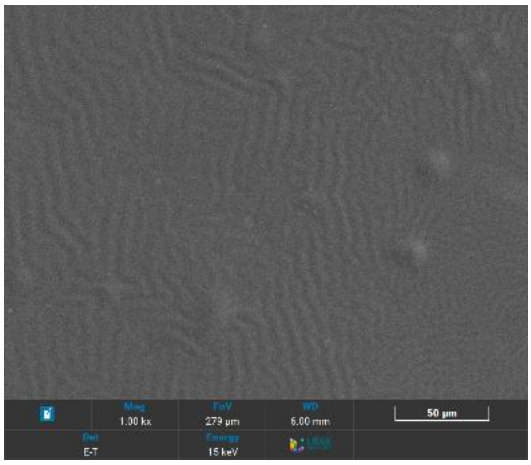

Figure 47: Image of aluminum foil with deposit in scanning electron microscopy (1000×).

Scanning electron microscopy does not show the presence of fibers, a layer of polymer rather appears to mask the roughness of the aluminum sheet surface, which would mean that there was no formation of nanofibers. Similar conclusion might be drawn from the optical microscopy images even if they show some differences between the aluminum sheet with deposit and the aluminum sheet alone. Indeed, in Figure 42 and 43, we observe that the aluminum alone is made up of continuous lines of the same diameter. The slight deviations of the lines observed in Figure 43 most certainly correspond to folds in the aluminum sheets. In Figure 40 and 41, on which we see the aluminum sheets with deposit, we observe continuous lines that also reflect light strongly sometimes, this is therefore

similar to an aluminum sheet.

However, these lines with larger diameters are very frequently encountered on an aluminum sheet with deposit while this was only observed only very few times during the multiple observation of aluminum sheet alone.

These different observations suggest that no nanofiber formation occurred, because even though the deposition observed under optical microscopy represents fibers, the diameter of the fiber is greater than 1000 nm given the scale.

The absence of nanofiber formation cannot be explained by a too slow fixation rate, as the collector is at -78°C, causing the PPEs to solidify instantly upon contact with the collector. During the UV irradiation time, they are fully crosslinked in about 2 minutes. The issue seems to stem from the fact that, under the electrospinning conditions used, the entanglement concentration was not reached, and therefore fiber formation did not occur. In the future, the focus should primarily be on the viscosity parameter of amorphous polyphosphoesters and on determining whether the entanglement concentration is reached for a pure amorphous PPE.

5. General conclusion

This thesis investigated the feasibility of producing amorphous PPEs nanofiber mats by electrospinning, addressing the challenges associated with their low glass transition temperature, which is below room temperature. The main objective was to optimize the experimental conditions to overcome the limitations of these viscous polymers, with a focus on their rheological behavior.

A comprehensive rheological analysis allowed to better determine the mechanical properties of PPEs. Viscosity measurements allowed to identify whether the pure PPEs studied are suitable for electrospinning, while the gel point time determined the feasibility of fixing the shape of PPEs during deposition. These results allowed to determine the strategies to be used to make nanofiber formation possible by electrospinning.

The results demonstrated that the studied PPEs, i.e. BenBP and BenHP, with molar masses ranging from 20,000 to 30,000 g/mol, and BenBP of approximately 70,000 g/mol, exhibited suitable viscosities for electrospinning without the addition of solvents. Gel point measurements indicated that photo-crosslinking in the presence of 5% photoinitiator occurs in approximately 1 minute and 29 seconds, suggesting that the solidification is too slow to prevent the polymer from flowing between the time the PPEs was deposited on the collector and the time it was completely solidified by photo-crosslinking.

For the solvent-free PPEs, electrospinning tests confirmed the formation of threads at the needle exit, but no threads were observed beyond the near-needle area. Therefore, I could not validate the suitability of the PPEs viscosity to the process. 3 solvent-based electrospinning tests were also performed with the studied PPEs, the observations showed the formation of drops at the needle outlet with solutions consisting of 10% by weight of THF. Consequently, the solvent-based electrospinning tests were directly abandoned. Concerning the deposition on the collector, given the low speed to reach the gel point, the collector was cooled to -78 ° C with dry ice, reducing the mobility of the PPEs by solidifying them instantly during deposition. Continuous photo-crosslinking during electrospinning ensured that all the structures formed remained fixed once the dry ice melted.

Finally, the infrared spectroscopy results indicated that the PPEs was successfully deposited on the collector and completely cross-linked. The results obtained by optical and electron microscopy allowed to conclude that no nanofiber formation occurred. This could be due to the fact that the entanglement concentration was not reached, which means that the pure polymer was not viscous enough. Consequently, in the future, it would be necessary to verify the hypothesis that the entanglement concentration is not reached for a pure amorphous polyphosphoester.

Although the goal of obtaining nanofibers was not achieved, this work represents an important first step in the search for a method to transform amorphous PPE into nanofiber mats.

6. Perspectives

This work opens up new perspectives by emphasizing the need to deepen studies on alternative approaches to achieve chain entanglement for the studied polyphosphoesters.

Indeed, as indicated in the results, the absence of nanofibers is likely due to insufficient chain entanglement. To confirm this hypothesis, it would first be necessary to determine the entanglement concentration by preparing various solutions at different concentrations using a suitable solvent or a mixture of solvents.

If the results indicate that this entanglement is insufficient to ensure fiber stability, several solutions can be considered. As detailed in the article by Ewaldz and Brettmann[62], various strategies based on molecular interactions can be employed to replace or complement traditional polymer chain entanglement. For instance, polymer-polymer interactions, such as hydrogen bonding or electrostatic interactions, can stabilize the electrospinning jet, even with low molecular weight polymers.

One alternative approach involves adding 1 to 5% by weight of a salt to the electrospinning solution, referencing studies such as those by Hisaschi Tee[40] and F. Cengiz et al.[43], which respectively demonstrated that adding 1,3-diaminopropane or tetraethylammonium bromide (TEAB) positively influences the formation of stable nanofibers.

Another potentially interesting approach is to electrospin the PPE solution with an electrospinnable semi-crystalline polymer in the presence of a solvent. This mixture would be electrospun under UV irradiation for one hour. The resulting nanofiber mat would then be dissolved in a solvent that is good for the semi-crystalline polymer and poor for the PPEs to recover only the PPE nanofibers. The theoretical principle behind this method involves both stabilization through polymer-polymer interactions, as explained earlier, and the fact that nanofibers scatter light in all directions, thereby accelerating the crosslinking rate of PPEs due to the presence of semi-crystalline polymer nanofibers.

Finally, this research into methods for processing amorphous PPEs into nanofiber mats

may also serve as a valuable foundation for 3D printing of PPEs, given the significant similarities between extrusion-based 3D printing processes and the electrospinning method in terms of the conditions required to transform polymers into nanofibers structures.

7. Annexes

7.1 NMR Spectra

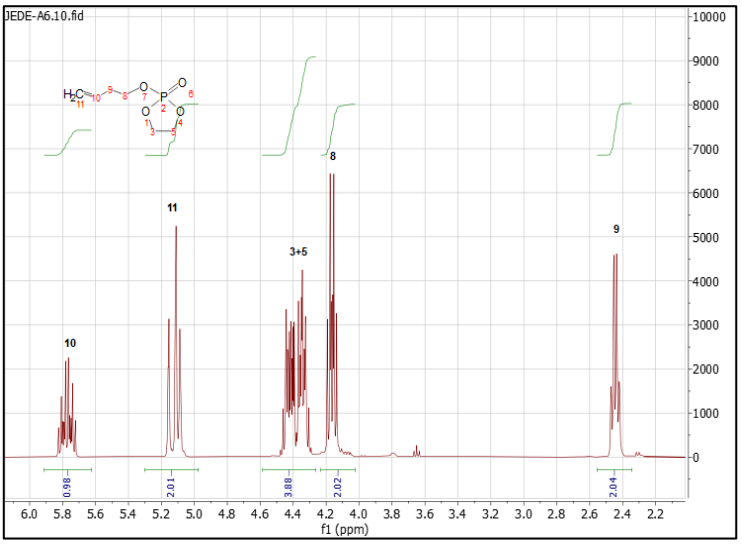

A1: RMN ^{1}H BenP monomer spectrum.

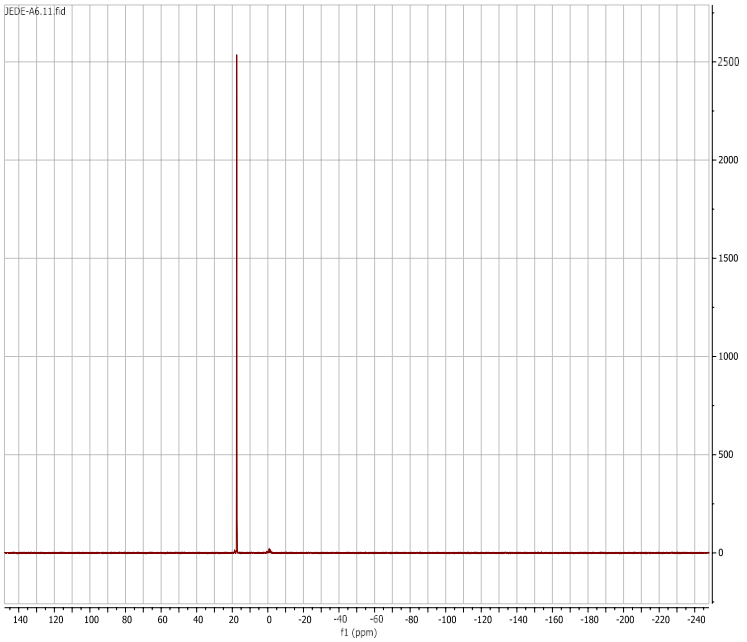

A2: NMR ^{31}P BenP monomer spectrum.

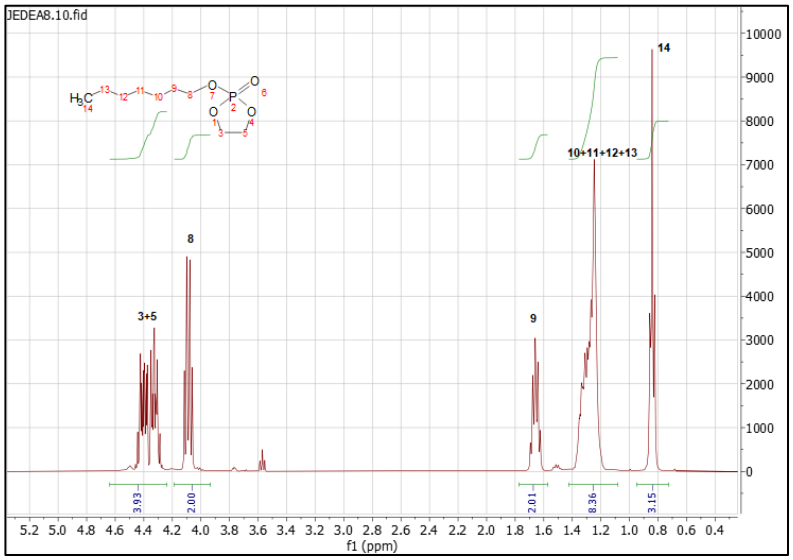

A3: NMR ^{1}H HP monomer spectrum.

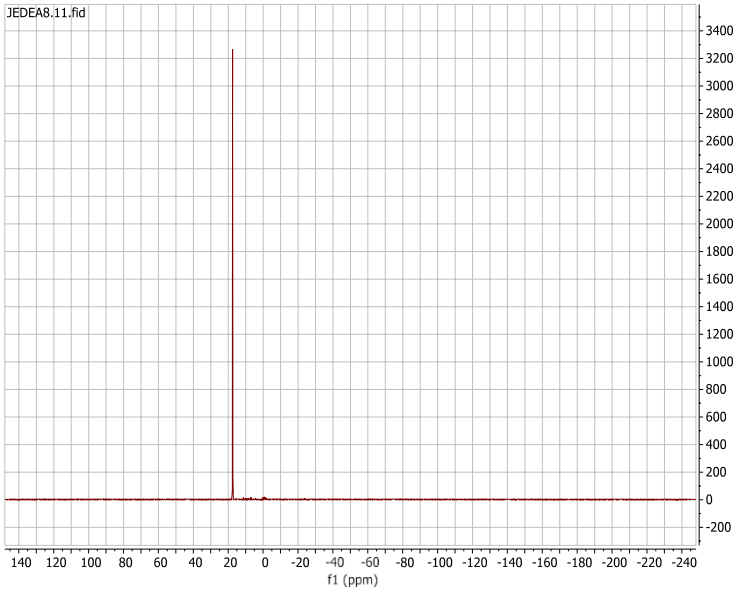

A4: NMR ^{31}P HP monomer spectrum.

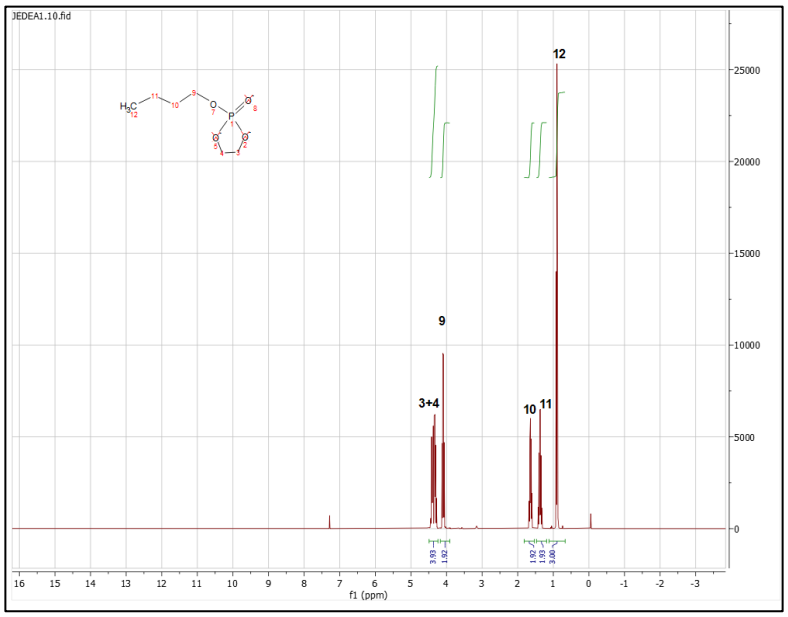

A5: NMR ^{1}H BP monomer spectrum.

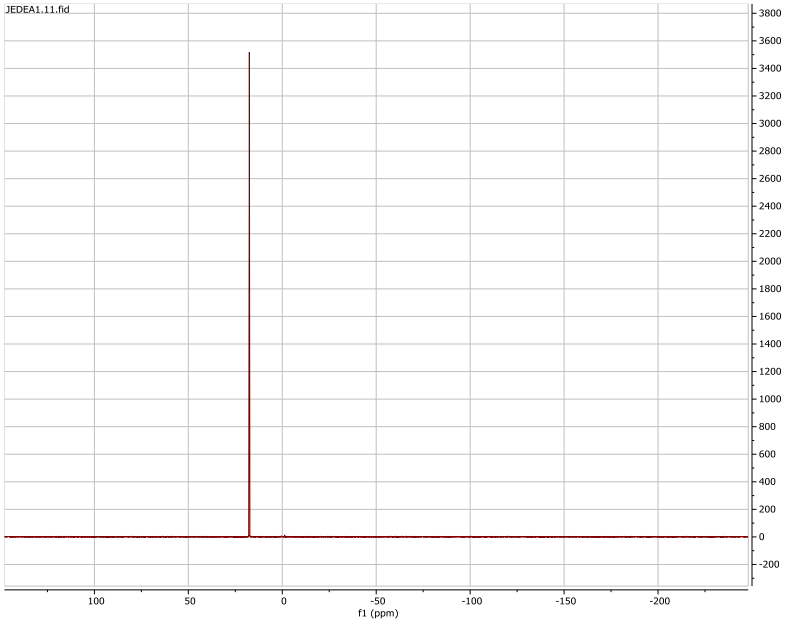

A6: NMR ^{31}P BP monomer spectrum.

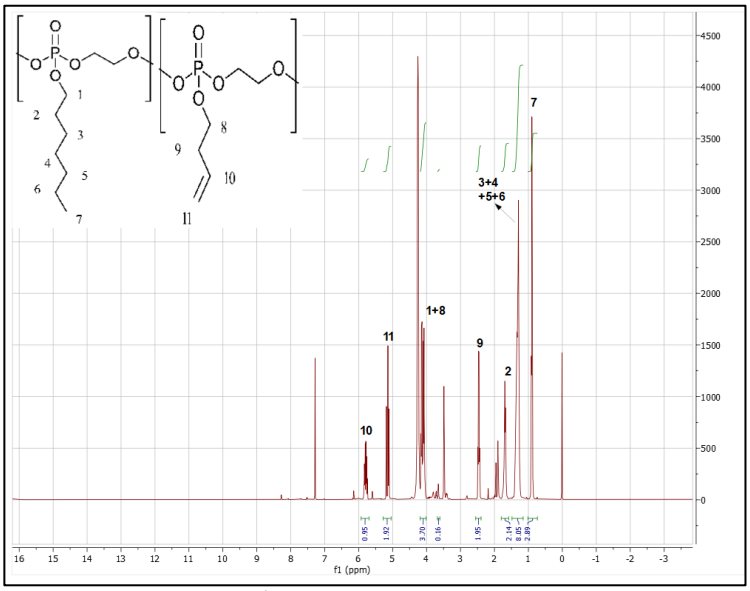

A7: NMR ^{1}H polymer BenHP spectrum.

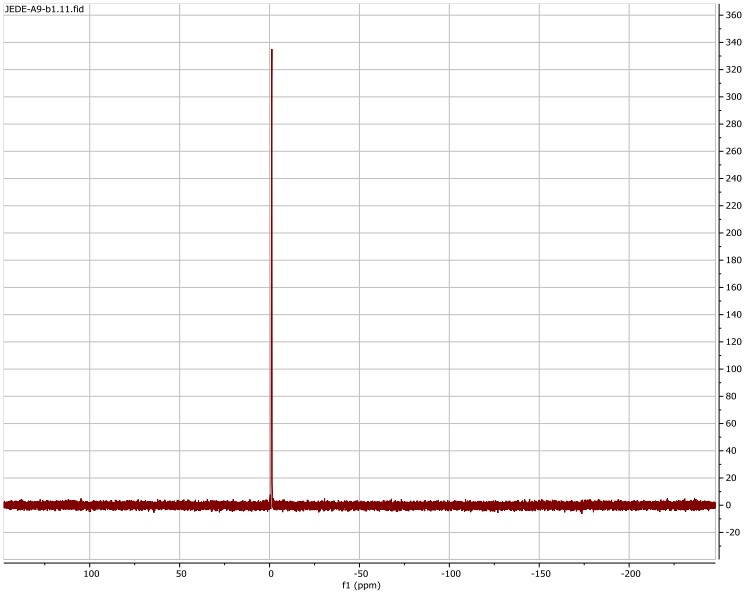

A8: NMR ^{31}P polymer BenHP spectrum.

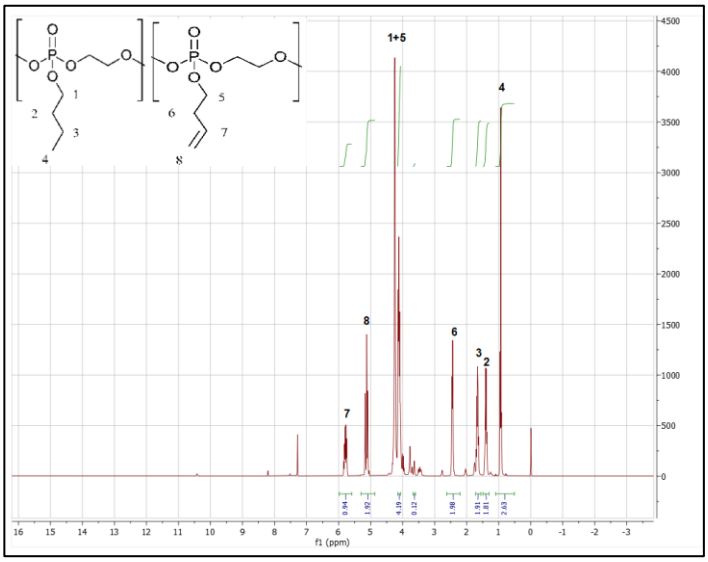

A9: NMR ^{1}H polymer BenBP spectrum.

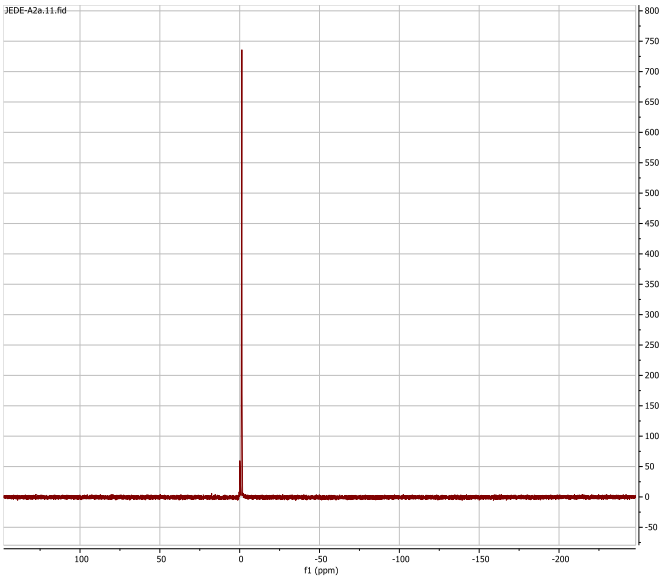

A10: NMR ^{31}P polymer BenBP spectrum.

7.2 GPC chromatogram

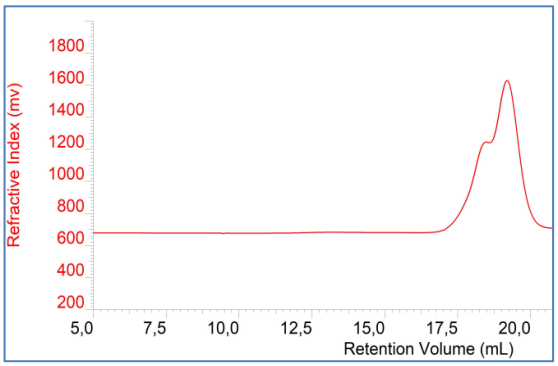

A11: GPC of polymer BenBP (25,954 g/mol).

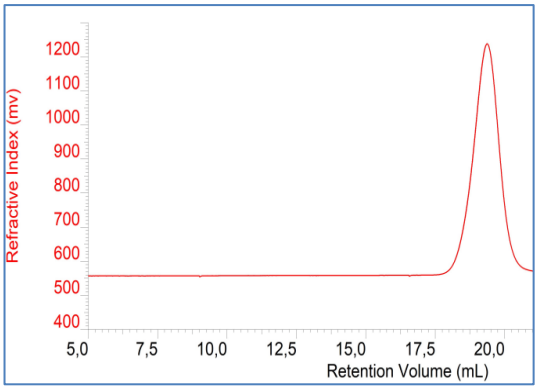

A12: GPC of polymer BenHP (26,121 g/mol).

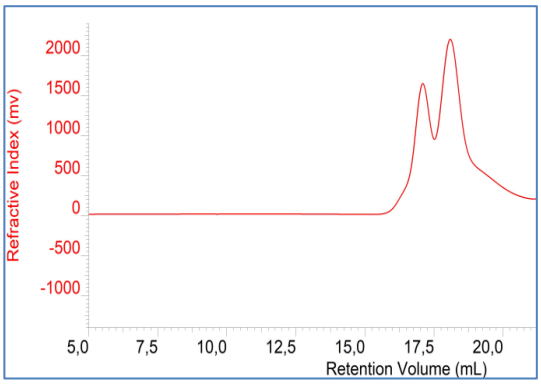

A13: GPC of polymer BenBP (74,432 g/mol).

7.3 Viscosity measure with rheometre ARES-G2

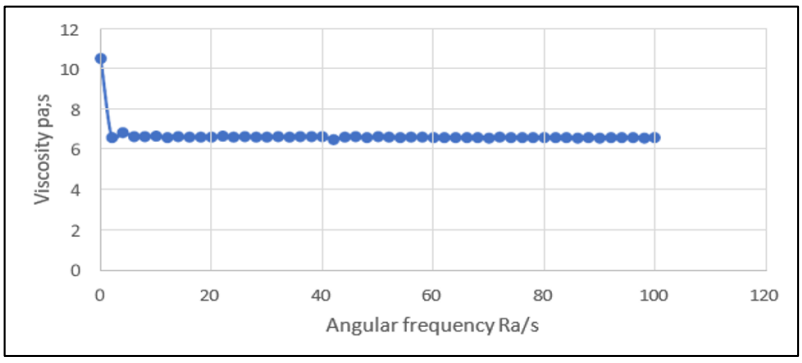

A14: Rheometer measurement of the complex viscosity of the statistical copolymer BenBP (22,600 g/mol) 100% previously dried empty. Average of the measurement: 6.65 Pa.s.

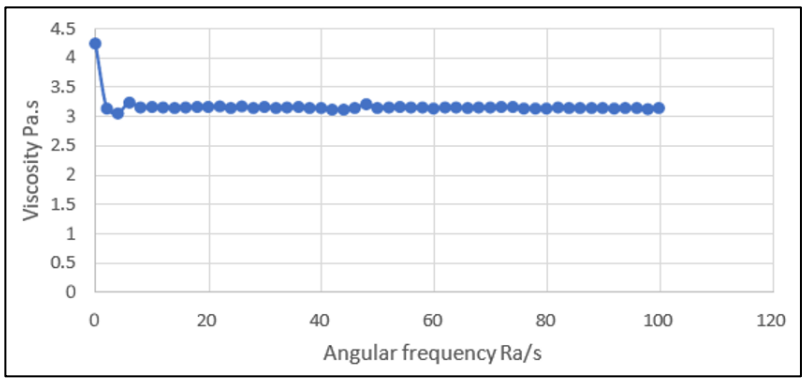

A15: Rheometer measurement of the complex viscosity of the statistical copolymer BenHP (22,069 g/mol) 100% previously dried empty.: Average of the measurement 3.14 Pa.s.

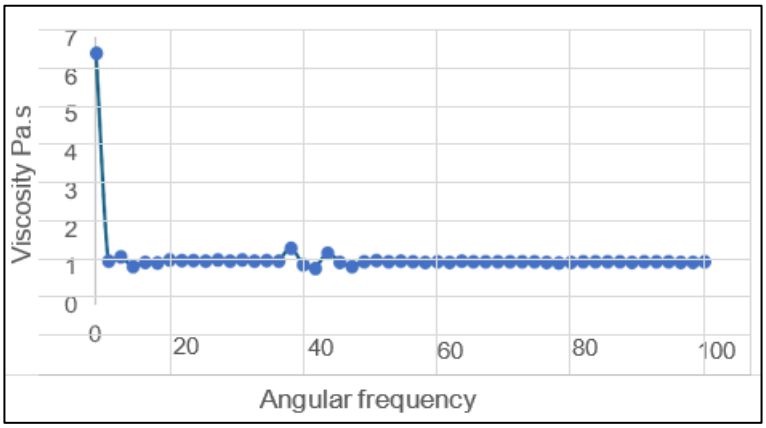

A16: Rheometer measurement of the complex viscosity of the statistical copolymer BenHP 100% previously dried under a hood. Average of the measurement: 1.15 Pa.s.

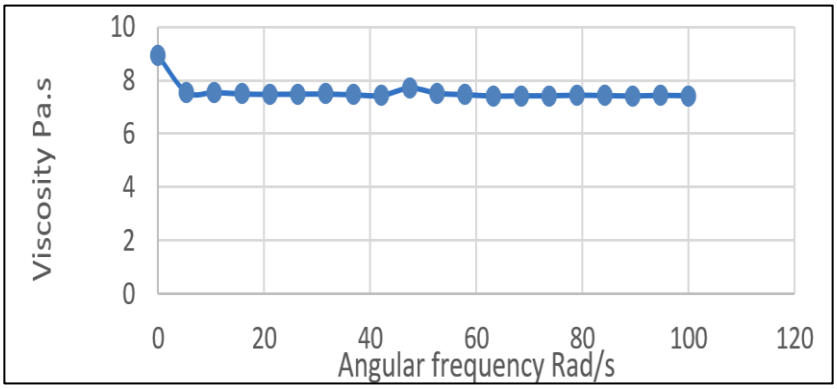

A17: Rheometer measurement of the complex viscosity of the statistical copolymer BenBP (~70,000 g/mol) 100% previously dried empty. Average of the measurement: 7.86 Pa.s.

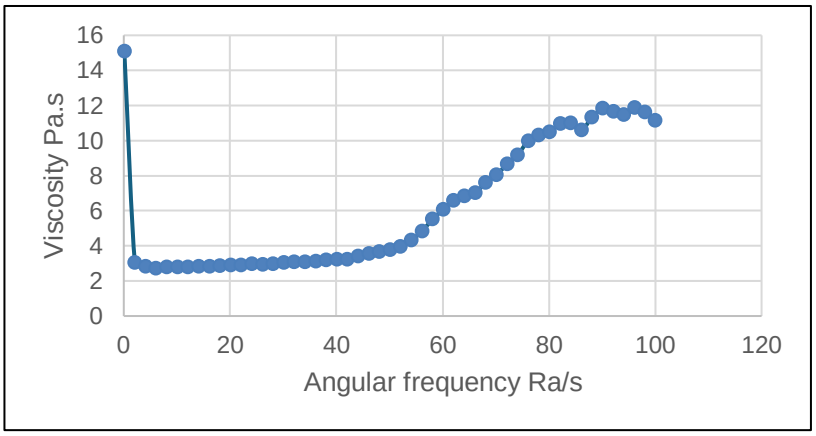

A18: Rheometer measurement of the complex viscosity of an electrospinnable solution of polycaprolactone. Average of the measurement: 2.95 Pa.s.

REFERENCES

[1] Ramakrishna S, Mayer J, Wintermantel E, Leong KW. Biomedical applications ofpolymer-composite materials: a review. Compos Sci Technol 2001; 61: 1189–224.

[2] Geckil H, Xu F, Zhang XH, Moon S, Demirci U. Engineering hydrogels as extracellularmatrix mimics. Nanomedicine 2010; 5:469–84.

[3] Rahmati M, Pennisi CP, Mobasheri A, Mozafari M. Bioengineered scaffolds for stem cell applications in tissue engineering and regenerative medicine. Adv Exp Med Biol 2018; 1107:73–89.

[4] Chapekar, M. S. (2000). Tissue engineering: Challenges and opportunities. Journal of Biomedical Materials Research, 53(6), 617–620. https://doi.org/10.1002/1097-4636(2000)53:6<617::AID-JBM1>3.0.CO; 2-C

[5] Feuerabendt, F., Nithitanakul, M., & Pakeyangkoon, P. (n.d.). Poly(HIPEs), Applications and Modifications. In International Journal of Engineering Research and Reviews (IJERR) (Vol. 2). www.researchpublish.com

[6] Smith, I. O., Liu, X. H., Smith, L. A., & Ma, P. X. (2009). Nanostructured polymer scaffolds for tissue engineering and regenerative medicine. 1, 226–236. https://doi.org/10.1002/wnan.026

[7] J. R. Fuchs, B. A. Nasseri, and J. P. Vacanti, "Tissue engineering: a 21st century solution to surgical reconstruction," Annals of Thoracic Surgery, vol. 72, no. 2, pp. 577–591, 2001.

[8] R. Langer and J. P. Vacanti, "Tissue engineering," Science, vol. 260, no. 5110, pp. 920– 926, 1993.

[9] R. Langer and D. A. Tirrell, "Designing materials for biology and medicine," Nature, vol. 428, no. 6982, pp. 487–492, 2004.

[10] Dhandayuthapani, B., Yoshida, Y., Maekawa, T., & Kumar, D. S. (2011). Polymeric scaffolds in tissue engineering application: A review. In International Journal of Polymer Science (Vol. 2011). Hindawi Limited. https://doi.org/10.1155/2011/290602

[11] A. S. Hoffman, "Hydrogels for biomedical applications," Annals of the New York Academy of Sciences, vol. 944, pp. 62– 73, 2001.

[12] Spicer, C. D. (2020). Hydrogel scaffolds for tissue engineering: The importance of polymer choice. In Polymer Chemistry (Vol. 11, Issue 2, pp. 184–219). Royal Society of Chemistry. https://doi.org/10.1039/c9py01021a

[13] Y. Du, H. Liu, Q. Yang et al., "Selective laser sintering scaffoldwith hierarchical architecture and gradient composition forosteochondral repair in rabbits," Biomaterials, vol. 137,pp. 37–48, 2017.

[14] Q. Zhang, H. Lu, N. Kawazoe, and G. Chen, "Pore size effectof collagen scaffolds oncartilage regeneration," Acta Bioma-terialia, vol. 10, no. 5, pp. 2005–2013, 2014.

[15] X. Li, J. Zhang, N. Kawazoe, and G. Chen, “Fabrication of highly crosslinked gelatin hydrogel and its influence on chon-drocyte proliferation and phenotype,” Polymers, vol. 9,no. 12, p. 309, 2017.

[16] Han, S., Nie, K., Li, J., Sun, Q., Wang, X., Li, X., & Li, Q. (2021). 3D ElectrospunNanofiber-Based Scaffolds: From Preparations and Properties to Tissue Regeneration Applications. In Stem Cells International (Vol. 2021). Hindawi Limited. https://doi.org/10.1155/2021/8790143

[17] Zhang, Y., Lim, C. T., Ramakrishna, S., & Huang, Z.-M. (n.d.). Recent development of polymer nanofibers for biomedical and biotechnological applications.

[18] P. X. Ma, “Scaffolds for tissue fabrication,” Materials Today, vol. 7, no. 5, pp. 30–40, 2004.

[19] Electrospinning-Electrospinning by Floriane LECLINCHE. (n.d.).

[20] Rahmati, M., Mills, D. K., Urbanska, A. M., Saeb, M. R., Venugopal, J. R., Ramakrishna, S., & Mozafari, M. (2021). Electrospinning for tissue engineering applications. In Progress in Materials Science (Vol. 117). Elsevier Ltd. https://doi.org/10.1016/j.pmatsci.2020.100721

[21] Tiwari, S. K., & Venkatraman, S. S. (2012). Importance of viscosity parameters in electrospinning: Of monolithic and core-shell fibers. Materials Science and Engineering C,32(5), 1037–1042. https://doi.org/10.1016/j.msec.2012.02.019

[22] McKee, M. G., Wilkes, G. L., Colby, R. H., & Long, T. E. (2004). Correlations of Solution Rheology with Electrospun Fiber Formation of Linear and Branched Polyesters. Macromolecules, 37(5), 1760–1767. https://doi.org/10.1021/ma035689h

[23]Gupta, P., Elkins, C., Long, T. E., & Wilkes, G. L. (2005). Electrospinning of linear homopolymers of poly(methyl methacrylate): Exploring relationships between fiber formation, viscosity, molecular weight and concentration in a good solvent. Polymer, 46(13),4799–4810. https://doi.org/10.1016/j.polymer.2005.04.021

[24] B. D. Fairbanks, M. P. Schwartz, C. N. Bowman and K. S. Anseth, Photoinitiated Polymerization of PEG-Diacrylate with Lithium Phenyl-2,4,6- Trimethylbenzoylphosphinate: Polymerization Rate and Cytocompatibility, Biomaterials, 2009, 30(35), 6702–6707.

[25] Willerth, S. M. (2017). Melt electrospinning in tissue engineering. In Electrospun Materials for Tissue Engineering and Biomedical Applications: Research, Design and Commercialization (pp. 87–100). Elsevier Inc. https://doi.org/10.1016/B978-0-08-101022-8.00009-0

[26] D. Li, Y.N. Xia, Electrospinning of nanofibers: Reinventing the wheel?, Adv. Mater. 16(2004) 1151–1170.

[27] Z.M. Huang, Y.Z. Zhang, M. Kotaki, S. Ramakrishna, A review on polymer nanofibersby electrospinning and their applications in nanocomposites, Compos. Sci. Technol. 63 (2003) 2223–2253.

[28] Y. Teo, S. Ramakrishna, A review on electrospinning design and nanofibre assemblies, Nanotechnology 17 (2006) 89–106.

[29] S. Ramakrishna, K. Fujihara, W.E. Teo, T.C. Lim, Z. Ma, An Introduction to Electrospinning

and Nanofibers, World Scientific Publishing Co., Singapore (2005).

[30] Hassounah, I.: 'Melt electrospinning of thermoplastic polymers'. 2012

[31] Valizadeh, A., & Farkhani, S. M. (2014). Electrospinning and electrospun nanofibres. IET Nanobiotechnology, 8(2), 83–92. https://doi.org/10.1049/iet-nbt.2012.0040

[32] Stansbury, J. W., & Idacavage, M. J. (2016). 3D printing with polymers: Challengesamong expanding options and opportunities. Dental Materials, 32(1), 54–64. https://doi.org/10.1016/j.dental.2015.09.018

[33] Rahmati, M., Mills, D. K., Urbanska, A. M., Saeb, M. R., Venugopal, J. R., Ramakrishna, S., & Mozafari, M. (2021). Electrospinning for tissue engineering applications. In Progress in Materials Science (Vol. 117). Elsevier Ltd. https://doi.org/10.1016/j.pmatsci.2020.100721

[34] Smith, I. O., Liu, X. H., Smith, L. A., & Ma, P. X. (2009). Nanostructured polymer scaffolds for tissue engineering and regenerative medicine. 1, 226–236. https://doi.org/10.1002/wnan.026

[35] Han, S., Nie, K., Li, J., Sun, Q., Wang, X., Li, X., & Li, Q. (2021). 3D Electrospun Nanofiber-Based Scaffolds: From Preparations and Properties to Tissue Regeneration Applications. In Stem Cells International (Vol. 2021). Hindawi Limited. https://doi.org/10.1155/2021/8790143

[36] Bini, T. B., Gao, S., Tan, T. C., Wang, S., Lim, A., Hai, L. ben, & Ramakrishna, S. (2004). Electrospun poly(L-lactide-co-glycolide) biodegradable polymer nanofibre tubes for peripheral nerve regeneration. Nanotechnology, 15(11), 1459–1464. https://doi.org/10.1088/0957-4484/15/11/014

[37] Alves Da Silva, M. L., Martins, A., Costa-Pinto, A. R., Costa, P., Faria, S., Gomes, M., Reis, R. L., & Neves, N. M. (2010). Cartilage tissue engineering using electrospun PCL nanofiber meshes and MSCs. Biomacromolecules, 11(12), 3228–3236. https://doi.org/10.1021/bm100476r

[38] Wang, Y. C., Yuan, Y. Y., Du, J. Z., Yang, X. Z., & Wang, J. (2009). Recent progress in polyphosphoesters: From controlled synthesis to biomedical applications. In Macromolecular Bioscience (Vol. 9, Issue 12, pp. 1154–1164). https://doi.org/10.1002/mabi.200900253

[39] Rheinberger, T., Rabaux, O., Jérôme, C., & Wurm, F. R. (2023). The future of polyphosphoesters. In European Polymer Journal (Vol. 200). Elsevier Ltd. https://doi.org/10.1016/j.eurpolymj.2023.112464

[40] Polyphosphoesters: A degradable alternative to polyolefins and poly(ethylene glycol). (n.d.).

[41] Shanmuganathan, K., Elliot, S. M., Lane, A. P., & Ellison, C. J. (2014). Highly stretchable thermoset fibers and nonwovens using thiol-ene photopolymerization. ACS Applied Materials and Interfaces, 6(16), 14259–14265. https://doi.org/10.1021/am503563q

[42] Jun, L., Zhang, Y., Hao, Y., Cheng, L., & Zhang, J. J. (2009). Preparation of porous electro-spun UPM fibers via photocrosslinking. Journal of Applied Polymer Science, 112(4), 2247–2254. https://doi.org/10.1002/app.29778

[43] s12221-009-0177-7. (n.d.).

[44] Design of self-folding shape-memory elastomer composites for biomedical applications. (n.d.).

[45] Ozdil, D., & Aydin, H. M. (2014). Polymers for medical and tissue engineering applications. In Journal of Chemical Technology and Biotechnology (Vol. 89, Issue 12, pp. 1793–1810). John

Wiley and Sons Ltd. https://doi.org/10.1002/jctb.4505

[46] P. Gunatillake, R. Mayadunne, and R. Adhikari, "Recent developments in biodegradable synthetic polymers," Biotechnology Annual Review, vol. 12, pp. 301–347, 2006.

[47] A.M. Reed, D.K. Gilding, Biodegradable polymers for use in surgery - poly(- glycolic)-poly(lactic acid) homo and co-polymers. 2. Invitro degradation, Polymer 22 (4) (1981) 494e498.

[48] Zhmayev, E., Cho, D., & Joo, Y. L. (2010). Modeling of melt electrospinning for semi-crystalline polymers. Polymer, 51(1), 274–290. https://doi.org/10.1016/j.polymer.2009.11.025

[49] Mondschein, R. J., Kanitkar, A., Williams, C. B., Verbridge, S. S., & Long, T. E. (2017). Polymer structure-property requirements for stereolithographic 3D printing of soft tissue engineering scaffolds. In Biomaterials (Vol. 140, pp. 170–188). Elsevier Ltd. https://doi.org/10.1016/j.biomaterials.2017.06.005

[50] Steinbach, T., & Wurm, F. R. (2015). Polyphosphoester: eine neue Plattform für abbaubare Polymere. Angewandte Chemie, 127(21), 6196–6207. https://doi.org/10.1002/ange.201500147

[51] Polyphosphoesters: A degradable alternative to polyolefins and poly(ethylene glycol). (n.d.).

[52] Riva, R., Shah, U., Thomassin, J. M., Yilmaz, Z., Lecat, A., Colige, A., & Jérôme, C. (2020). Design of Degradable Polyphosphoester Networks with Tailor-Made Stiffness and Hydrophilicity as Scaffolds for Tissue Engineering. Biomacromolecules, 21(2), 349–355. https://doi.org/10.1021/acs.biomac.9b01276

[53] J. Pretula, S. Penczek, Poly (ethylene glycol) ionomers with phosphate diester linkages, Makromol. Chem. Rapid 9 (11) (1988) 731–737.

[54] Iliescu, S., Avram, E., Visa, A., Plesu, N., Popa, A., & Ilia, G. (2011). New technique forthe synthesis of polyphosphoesters. Macromolecular Research, 19(11), 1186–1191. https://doi.org/10.1007/s13233-011-1111-6

[55] Steinbach, T., Alexandrino, E. M., & Wurm, F. R. (2013). Unsaturated poly(phosphoester)s via ring-opening metathesis polymerization. Polymer Chemistry, 4(13), 3800–3806. https://doi.org/10.1039/c3py00437f

[56] H.T. Tee, K. Koynov, T. Reichel, F.R. Wurm, Noncovalent Hydrogen Bonds Tune the Mechanical Properties of Phosphoester Polyethylene Mimics, ACS Omega 4 (5) (2019) 9324–9332.

[57] Clément, B., Grignard, B., Koole, L., Jéroîme, C., & Lecomte, P. (2012). Metal-freestrategies for the synthesis of functional and well-defined polyphosphoesters.
Macromolecules, 45(11), 4476–4486. https://doi.org/10.1021/ma3004339

[58] Yilmaz, Z. E., & Jérôme, C. (2016). Polyphosphoesters: New Trends in Synthesis and Drug Delivery Applications. Macromolecular Bioscience, 16(12), 1745–1761. https://doi.org/10.1002/mabi.201600269

[59] Jérôme, C., & Lombardi, M. (n.d.). Polyphosphoester elastomers: A syntheticinvestigation towards improved elastic properties.

[60] Author, 7, Mukhopadhyay, A. K., & Jang, S. (2008). USING CEMENT PASTE RHEOLOGY TO PREDICT CONCRETE MIX DESIGN PROBLEMS: TECHNICAL REPORT

5. Report Date 6. Performing Organization Code Project 0-5820 13. Type of Report and Period Covered Project performed in cooperation with the Texas Department of Transportation and the Federal Highway Administration. Project Title: Using Cement PasteRheology to Predict Concrete Mix Design Problems Unclassified.

[61] THE_STRUCTURE_AND_RHEOLOGY_OF_COMPLEX_FL (1). (n.d.).

[62] Ewaldz, E., & Brettmann, B. (2019). Molecular Interactions in Electrospinning: From Polymer Mixtures to Supramolecular Assemblies. In *ACS Applied Polymer Materials* (Vol. 1, Issue 3, pp. 298–308). American Chemical Society. https://doi.org/10.1021/acsapm.8b00073